Mesure du chaos

Haris Skokos

Astronomie et Systèmes Dynamiques, IMCCE,
Observatoire de Paris, Paris, France

E-mail: hskokos@imcce.fr

URL: http://www.imcce.fr/~hskokos/

Outline

- Basic concepts of Hamiltonian systems and symplectic maps
  - ✓ Poincaré Surface of Section
  - ✓ Variational equations
  - ✓ Lyapunov exponents
  - ✓ Chaos detection techniques
- Smaller ALignment Index – SALI
  - ✓ Definition
  - ✓ Behavior for chaotic and regular motion
  - ✓ Applications
- Generalized ALignment Index – GALI
  - ✓ Definition - Relation to SALI
  - ✓ Behavior for chaotic and regular motion
  - ✓ Applications
  - ✓ Global dynamics

Autonomous Hamiltonian systems

Consider an N degree of freedom autonomous Hamiltonian system having a Hamiltonian function of the form:

$$H(\overbrace{q_1,q_2,\ldots,q_N}^{\text{positions}}, \overbrace{p_1,p_2,\ldots,p_N}^{\text{momenta}})$$

The time evolution of an orbit (trajectory) with initial condition

$$P(0)=(q_1(0), q_2(0),\ldots,q_N(0), p_1(0), p_2(0),\ldots,p_N(0))$$

is governed by the Hamilton's equations of motion

$$\frac{dp_i}{dt} = -\frac{\partial H}{\partial q_i} \quad , \quad \frac{dq_i}{dt} = \frac{\partial H}{\partial p_i}$$

Poincaré Surface of Section (PSS)

We can constrain the study of an N+1 degree of freedom Hamiltonian system to a 2N-dimensional subspace of the general phase space.

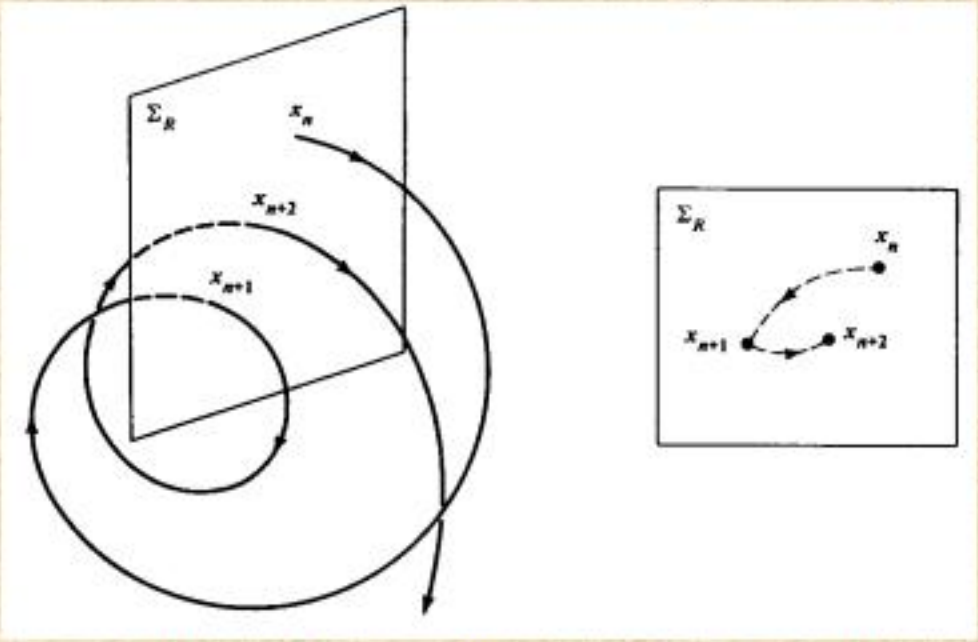

Lieberman & Lichtenberg, 1992, *Regular and Chaotic Dynamics*, Springer.

In general we can assume a PSS of the form q_{N+1}=constant. Then only variables $q_1,q_2,\ldots,q_N,p_1,p_2,\ldots,p_N$ are needed to describe the evolution of an orbit on the PSS, since p_{N+1} can be found from the Hamiltonian.

In this sense an N+1 degree of freedom Hamiltonian system corresponds to a 2N-dimensional symplectic map.

Variational Equations

We use the notation $x = (q_1,q_2,\ldots,q_N,p_1,p_2,\ldots,p_N)^T$. The **deviation vector** from a given orbit is denoted by

$$v = (dx_1, dx_2,\ldots, dx_n)^T \text{ , with } n=2N$$

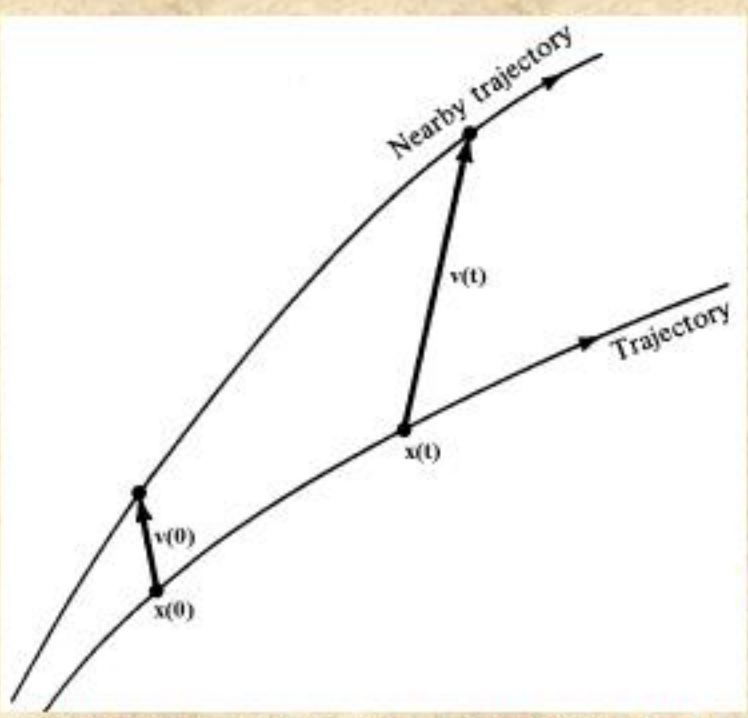

Benettin & Galgani, 1979, in Laval and Gressillon (eds.), op cit, 93

The time evolution of v is given by the so-called **variational equations:**

$$\frac{dv}{dt} = -J \cdot P \cdot v$$

where

$$J = \begin{pmatrix} 0_N & -I_N \\ I_N & 0_N \end{pmatrix}, \quad P_{ij} = \frac{\partial^2 H}{\partial x_i \partial x_j} \quad i,j = 1,2,\ldots,n$$

Example (Hénon-Heiles system)

$$H = \frac{1}{2}\left(p_x^2 + p_y^2\right) + \frac{1}{2}\left(x^2 + y^2\right) + x^2 y - \frac{1}{3}y^3$$

Hamilton's equations of motion:

$$\frac{dp_i}{dt} = -\frac{\partial H}{\partial q_i}\,,\ \frac{dq_i}{dt} = \frac{\partial H}{\partial p_i} \Rightarrow \begin{cases} \dot{x} = p_x \\ \dot{y} = p_y \\ \dot{p}_x = -x - 2xy \\ \dot{p}_y = -y - x^2 + y^2 \end{cases}$$

In order to get the variational equations we linearize the above equations by substituting x, y, px, py with $x+v_1$, $y+v_2$, p_x+v_3, p_y+v_4 where $v=(v_1,v_2,v_3,v_4)$ is the deviation vector. So we get:

$$\dot{p}_x + \dot{v}_3 = -x - v_1 - 2(x+v_1)(y+v_2) \Rightarrow$$

$$\dot{p}_x + \dot{v}_3 = -x - v_1 - 2xy - 2xv_2 - 2yv_1 - 2v_1v_2 \Rightarrow$$

$$\dot{v}_3 = -v_1 - 2yv_1 - 2xv_2$$

Example (Hénon-Heiles system)

Variational equations: $\dfrac{dv}{dt} = -J \cdot P \cdot v$

$$\begin{pmatrix} \dot{v}_1 \\ \dot{v}_2 \\ \dot{v}_3 \\ \dot{v}_4 \end{pmatrix} = - \begin{pmatrix} 0 & 0 & -1 & 0 \\ 0 & 0 & 0 & -1 \\ 1 & 0 & 0 & 0 \\ 0 & 1 & 0 & 0 \end{pmatrix} \begin{pmatrix} 1+2y & 2x & 0 & 0 \\ 2x & 1-2y & 0 & 0 \\ 0 & 0 & 1 & 0 \\ 0 & 0 & 0 & 1 \end{pmatrix} \begin{pmatrix} v_1 \\ v_2 \\ v_3 \\ v_4 \end{pmatrix}$$

$$\begin{aligned} \dot{v}_1 &= v_3 \\ \dot{v}_2 &= v_4 \\ \dot{v}_3 &= -v_1 - 2xv_2 - 2yv_1 \\ \dot{v}_4 &= -v_2 - 2xv_1 + 2yv_2 \end{aligned} \quad + \quad \begin{aligned} \dot{x} &= p_x \\ \dot{y} &= p_y \\ \dot{p}_x &= -x - 2xy \\ \dot{p}_y &= -y - x^2 + y^2 \end{aligned}$$

Complete set of equations

Symplectic Maps

Consider an n-dimensional symplectic map T. In this case we have discrete time.

The evolution of an orbit with initial condition

$$P(0)=(x_1(0), x_2(0),\ldots,x_n(0))$$

is governed by the equations of map T

$$P(i+1)=T\,P(i)\ ,\ i=0,1,2,\ldots$$

The evolution of an initial deviation vector

$$v(0) = (dx_1(0), dx_2(0),\ldots, dx_n(0))$$

is given by the corresponding tangent map

$$v(i+1) = \left.\frac{\partial T}{\partial P}\right|_i \cdot v(i)\ ,\ i = 0,1,2,\ldots$$

Example – 2D map

Equations of the map:

$$\begin{pmatrix} x_1' \\ x_2' \end{pmatrix} = T\begin{pmatrix} x_1 \\ x_2 \end{pmatrix} \Rightarrow \begin{aligned} x_1' &= x_1 + x_2 \\ x_2' &= x_2 - \nu \sin(x_1 + x_2) \end{aligned} \qquad (\mathrm{mod}\ 2\pi)$$

Tangent map:

$$v(i+1) = \left.\frac{\partial T}{\partial P}\right|_i \cdot v(i)$$

$$\begin{pmatrix} dx_1' \\ dx_2' \end{pmatrix} = \begin{pmatrix} 1 & 1 \\ -\nu\cos(x_1 + x_2) & 1 - \nu\cos(x_1 + x_2) \end{pmatrix} \begin{pmatrix} dx_1 \\ dx_2 \end{pmatrix}$$

Chaos detection methods

- **Analysis of the orbit under study**
  - ✓ **Frequency Analysis**
  - ✓ **Low frequency power (LFP)**
  - ✓ **0-1 test**
  - ✓ **Patterns method**

- **Study of the evolution of deviation vectors**
  - ✓ **Lyapunov exponents**
  - ✓ **SALI – GALI$_k$**
  - ✓ **Fast Lyapunov Indicator (FLI) and its variants**
  - ✓ **Mean exponential growth of nearby orbits (MEGNO)**
  - ✓ **Relative Lyapunov Indicator (RLI)**
  - ✓ **Dynamical Spectra**

Lyapunov Exponents

Roughly speaking, the Lyapunov exponents of a given orbit characterize the mean exponential rate of divergence of trajectories surrounding it.

Consider an orbit in an M-dimensional phase space with initial condition x(0) and an initial deviation vector from it v(0). Then the mean exponential rate of divergence is:

$$\sigma(x(0), v(0)) = \lim_{t \to \infty} \frac{1}{t} \ln \frac{\|v(t)\|}{\|v(0)\|}$$

Lyapunov Exponents

There exists an M-dimensional basis $\{\hat{e}_i\}$ of v such that for any v, σ takes one of the M (possibly nondistinct) values

$$\sigma_i(x(0)) = \sigma(x(0), \hat{e}_i)$$

which are the Lyapunov exponents.

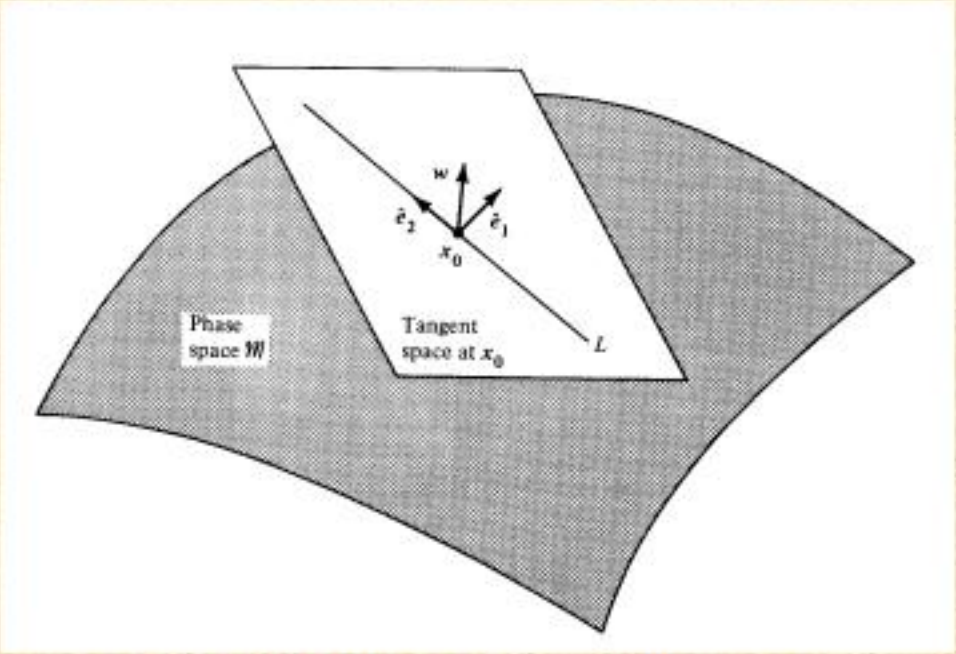

Benettin & Galgani, 1979, in Laval and Gressillon (eds.), op cit, 93

In autonomous Hamiltonian systems the M exponents are ordered in pairs of opposite sign numbers and two of them are 0.

Computation of the Maximal Lyapunov Exponent

Due to the exponential growth of v(t) (and of d(t)=||v(t)||) we renormalize v(t) from time to time.

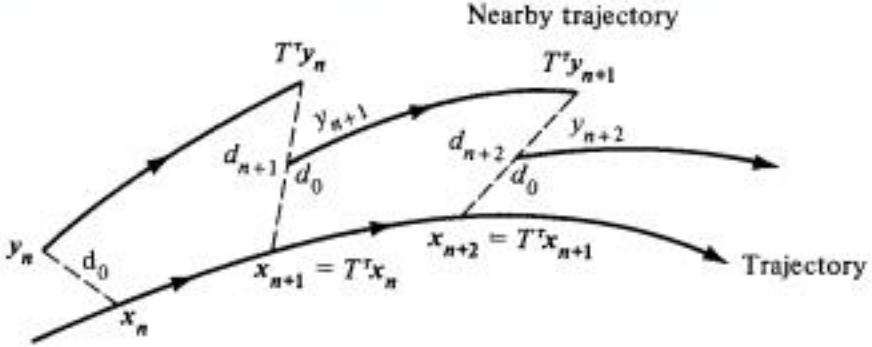

Figure 5.6. Numerical calculation of the maximal Liapunov characteristic exponent. Here $y = x + v$ and τ is a finite interval of time (after Benettin *et al.*, 1976).

Then the Maximal Lyapunov exponent is computed as

$$\sigma_1 = \lim_{n\to\infty} \frac{1}{n\tau} \sum_{i=1}^{n} \ln d_i$$

Maximal Lyapunov Exponent

$\sigma_1=0 \rightarrow$ Regular motion

$\sigma_1\neq0 \rightarrow$ Chaotic motion

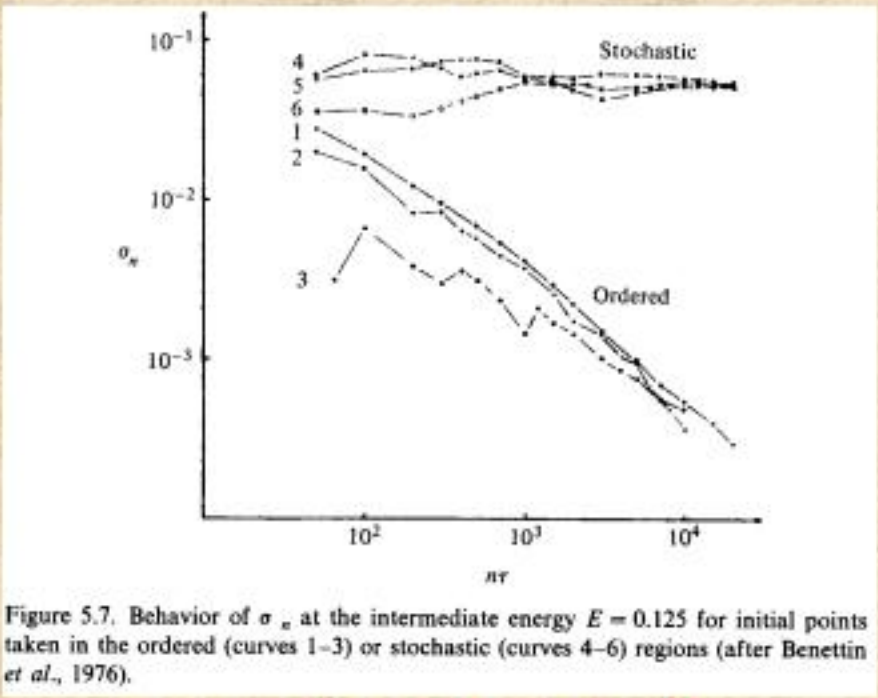

Figure 5.7. Behavior of σ_n at the intermediate energy $E = 0.125$ for initial points taken in the ordered (curves 1–3) or stochastic (curves 4–6) regions (after Benettin *et al.*, 1976).

Benettin et al. (1980) proposed an algorithm for the computation of all Lyapunov exponents.

Over the years several methods for the computation of few Lyapunov exponents have been developed (e.g. Greene & Kim 1987, Bridges & Reich 2001).

Frequency Analysis

We compute the fundamental frequencies of an orbit using the NAFF (Numerical Analysis of the Fundamental Frequency) algorithm (Laskar 1988).

Frequency Maps

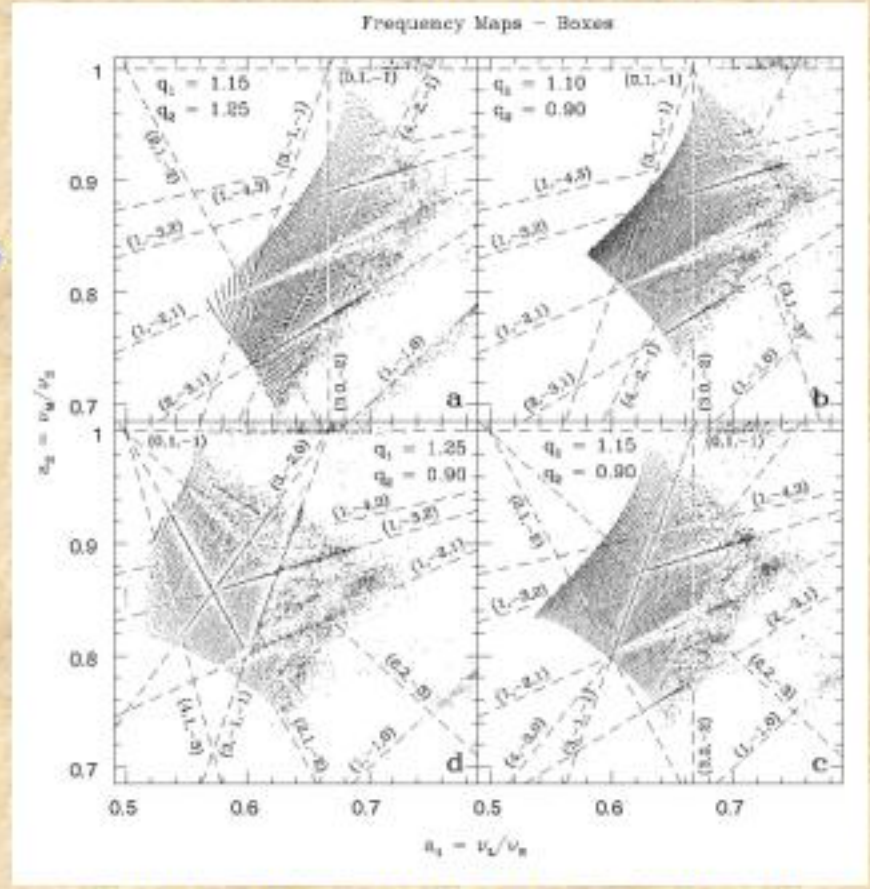

Papaphilippou Y and Laskar J 1998 Astron. Astrophys. 329 451

Regular motion : The computed frequencies do not vary in time

Chaotic motion : The computed frequencies vary in time

Frequency Analysis

Stability of Trojan asteroids, (α, e) diagram (Robutel & Gabern 2006)

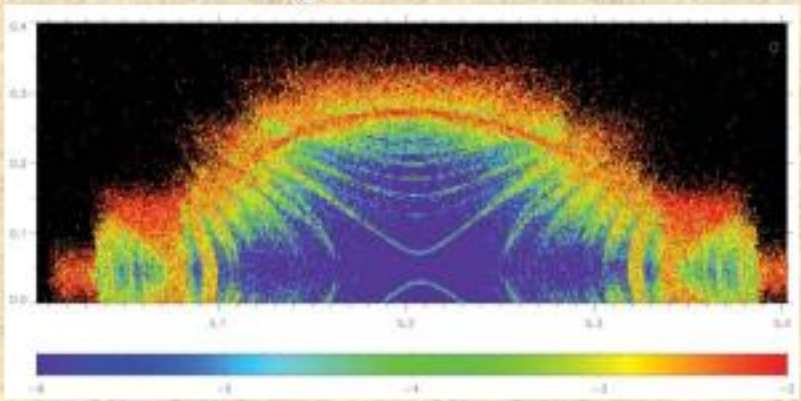

Dynamics of ESRF storage ring

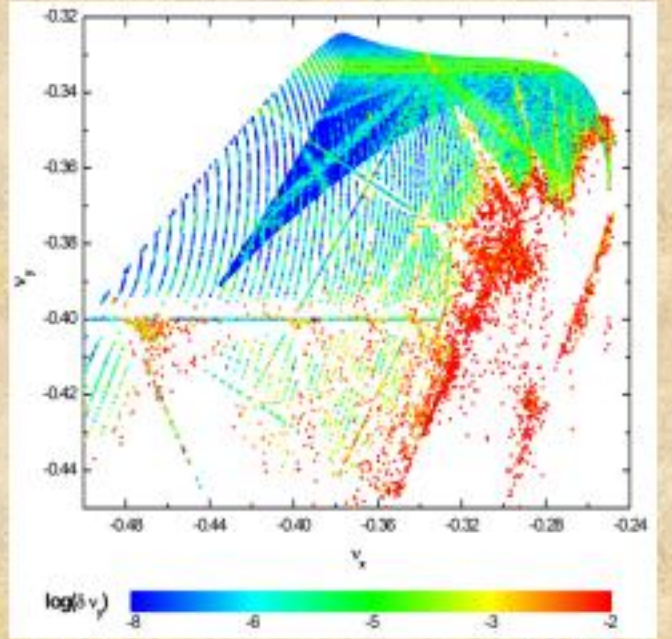

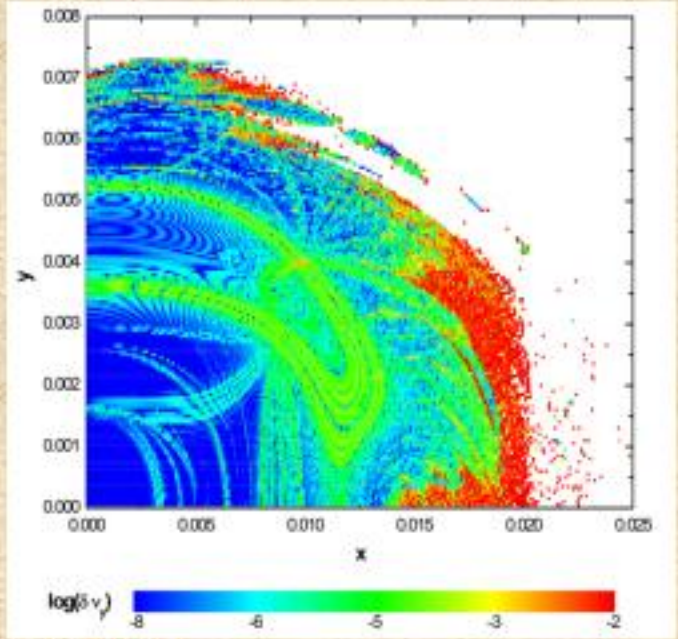

The Smaller ALignment Index (SALI) method

Definition of Smaller Alignment Index (SALI)

Consider the n-dimensional phase space of a conservative dynamical system (symplectic map or Hamiltonian flow).

An orbit in that space with initial condition :

$$P(0)=(x_1(0), x_2(0),\ldots,x_n(0))$$

and a deviation vector

$$v(0)=(dx_1(0), dx_2(0),\ldots, dx_n(0))$$

The evolution in time (in maps the time is discrete and is equal to the number N of the iterations) of a deviation vector is defined by:

- the variational equations (for Hamiltonian flows) and
- the equations of the tangent map (for mappings)

Definition of SALI

We follow the evolution in time of two different initial deviation vectors $(v_1(0), v_2(0))$, and define SALI (Skokos, 2001, J. Phys. A) as:

$$SALI(t) = \min\left\{\left\|\hat{v}_1(t) + \hat{v}_2(t)\right\|, \left\|\hat{v}_1(t) - \hat{v}_2(t)\right\|\right\}$$

where

$$\hat{v}_1(t) = \frac{v_1(t)}{\left\|v_1(t)\right\|}$$

When the two vectors become collinear

$$SALI(t) \rightarrow 0$$

Behavior of SALI for chaotic motion

For chaotic orbits the two initially different deviation vectors tend to coincide with the direction defined by the maximal Lyapunov exponent.

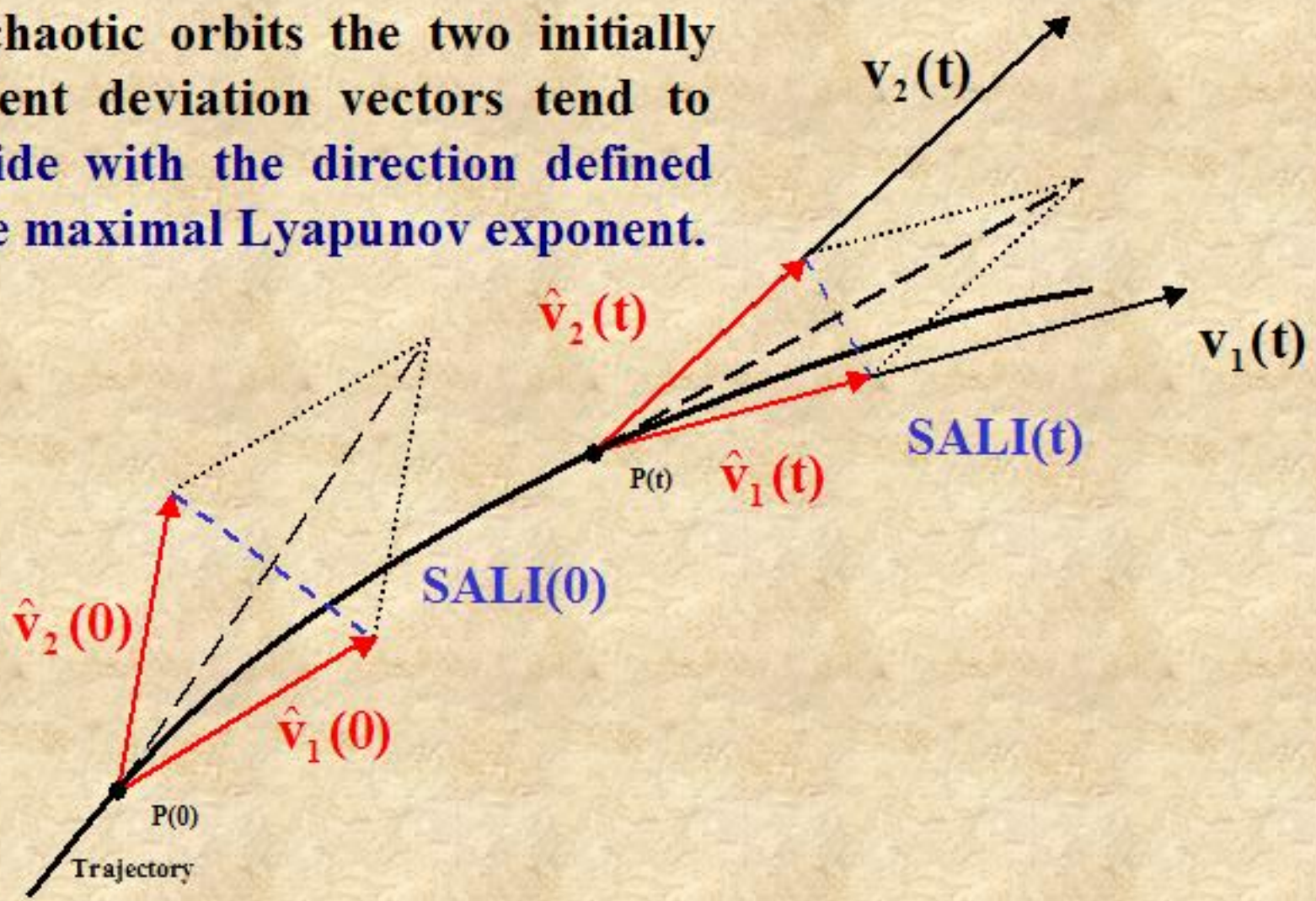

Behavior of SALI for chaotic motion

The evolution of a deviation vector can be approximated by:

$$\mathbf{v}_1(t) = \sum_{i=1}^{n} c_i^{(1)} e^{\sigma_i t} \hat{\mathbf{u}}_i \approx c_1^{(1)} e^{\sigma_1 t} \hat{\mathbf{u}}_1 + c_2^{(1)} e^{\sigma_2 t} \hat{\mathbf{u}}_2$$

where $\sigma_1 > \sigma_2 \geq \ldots \geq \sigma_n$ are the Lyapunov exponents.

In this approximation, we derive a leading order estimate of the ratio

$$\frac{\mathbf{v}_1(t)}{\|\mathbf{v}_1(t)\|} \approx \frac{c_1^{(1)} e^{\sigma_1 t} \hat{\mathbf{u}}_1 + c_2^{(1)} e^{\sigma_2 t} \hat{\mathbf{u}}_2}{\left|c_1^{(1)}\right| e^{\sigma_1 t}} = \pm \hat{\mathbf{u}}_1 + \frac{c_2^{(1)}}{\left|c_1^{(1)}\right|} e^{-(\sigma_1 - \sigma_2)t} \hat{\mathbf{u}}_2$$

and an analogous expression for $\mathbf{v}_2$

$$\frac{\mathbf{v}_2(t)}{\|\mathbf{v}_2(t)\|} \approx \frac{c_1^{(2)} e^{\sigma_1 t} \hat{\mathbf{u}}_1 + c_2^{(2)} e^{\sigma_2 t} \hat{\mathbf{u}}_2}{\left|c_1^{(2)}\right| e^{\sigma_1 t}} = \pm \hat{\mathbf{u}}_1 + \frac{c_2^{(2)}}{\left|c_1^{(2)}\right|} e^{-(\sigma_1 - \sigma_2)t} \hat{\mathbf{u}}_2$$

So we get:

$$\mathrm{SALI}(t) = \min\left\{ \left\| \frac{\mathbf{v}_1(t)}{\|\mathbf{v}_1(t)\|} + \frac{\mathbf{v}_2(t)}{\|\mathbf{v}_2(t)\|} \right\|, \left\| \frac{\mathbf{v}_1(t)}{\|\mathbf{v}_1(t)\|} - \frac{\mathbf{v}_2(t)}{\|\mathbf{v}_2(t)\|} \right\| \right\} \approx \left| \frac{c_2^{(1)}}{\left|c_1^{(1)}\right|} \pm \frac{c_2^{(2)}}{\left|c_1^{(2)}\right|} \right| e^{-(\sigma_1 - \sigma_2)t}$$

Behavior of SALI for chaotic motion

We test the validity of the approximation $SALI \propto e^{-(\sigma 1-\sigma 2)t}$ (Skokos et al., 2004, J. Phys. A) for a chaotic orbit of the 3D Hamiltonian

$$H = \sum_{i=1}^{3} \frac{\omega_i}{2}(q_i^2 + p_i^2) + q_1^2 q_2 + q_1^2 q_3$$

with $\omega_1=1$, $\omega_2=1.4142$, $\omega_3=1.7321$, $H=0.09$

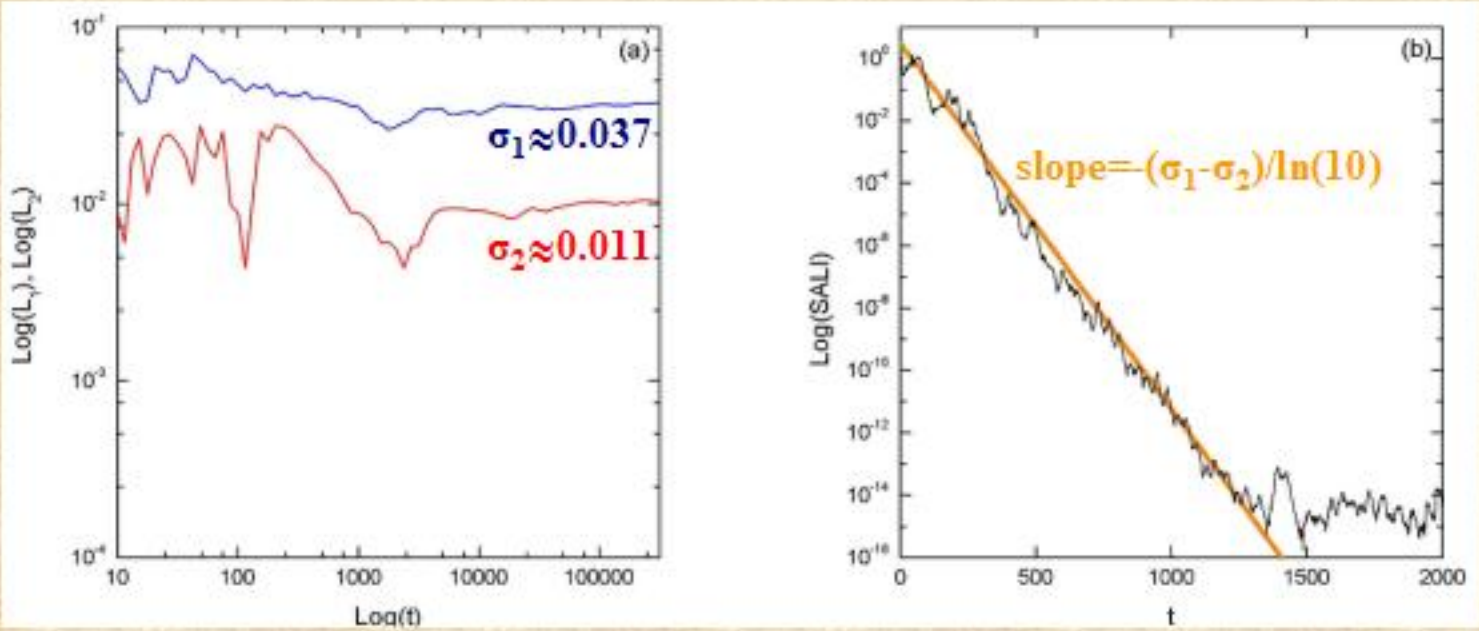

Behavior of SALI for regular motion

Regular motion occurs on a torus and two different initial deviation vectors become tangent to the torus, generally having different directions.

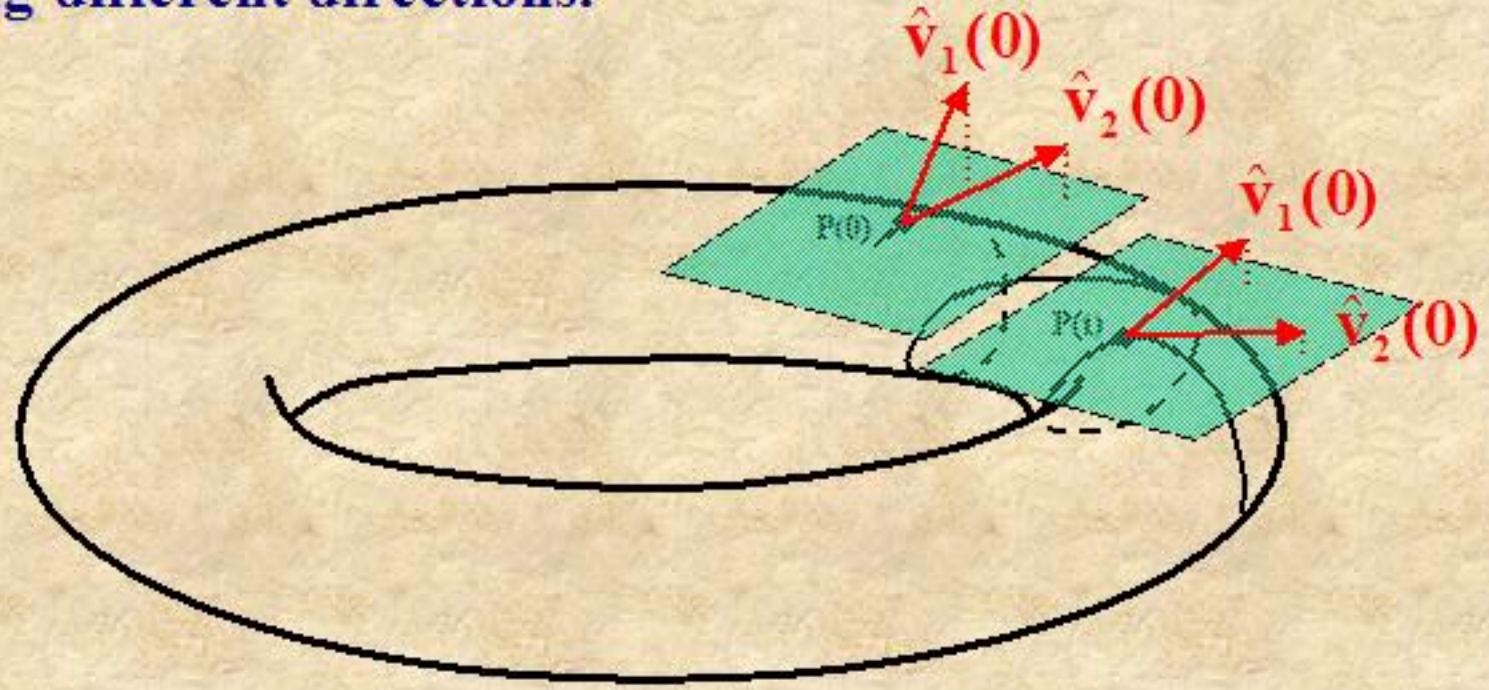

Applications – Hénon-Heiles system

For E=1/8 we consider the orbits with initial conditions:
Ordered orbit, x=0, y=0.55, p_x=0.2417, p_y=0
Chaotic orbit, x=0, y=-0.016, p_x=0.49974, p_y=0
Chaotic orbit, x=0, y=-0.01344, p_x=0.49982, p_y=0

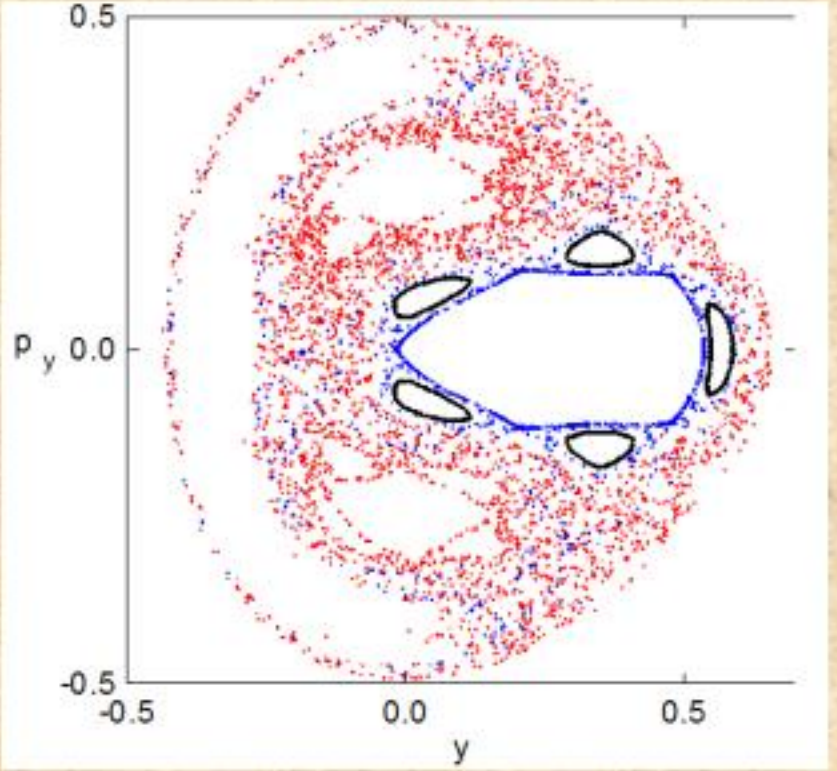

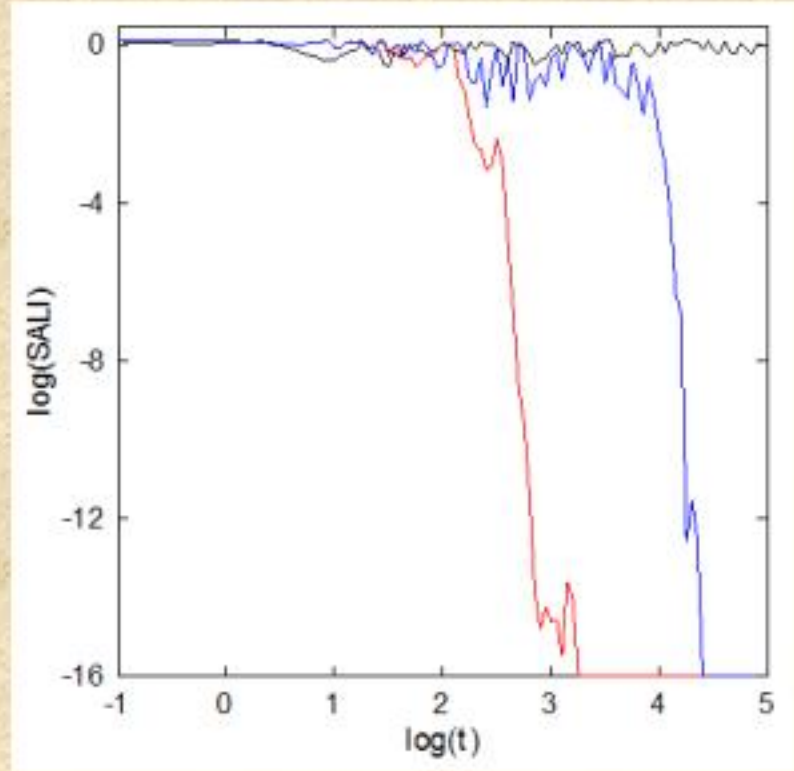

Applications – Hénon-Heiles system

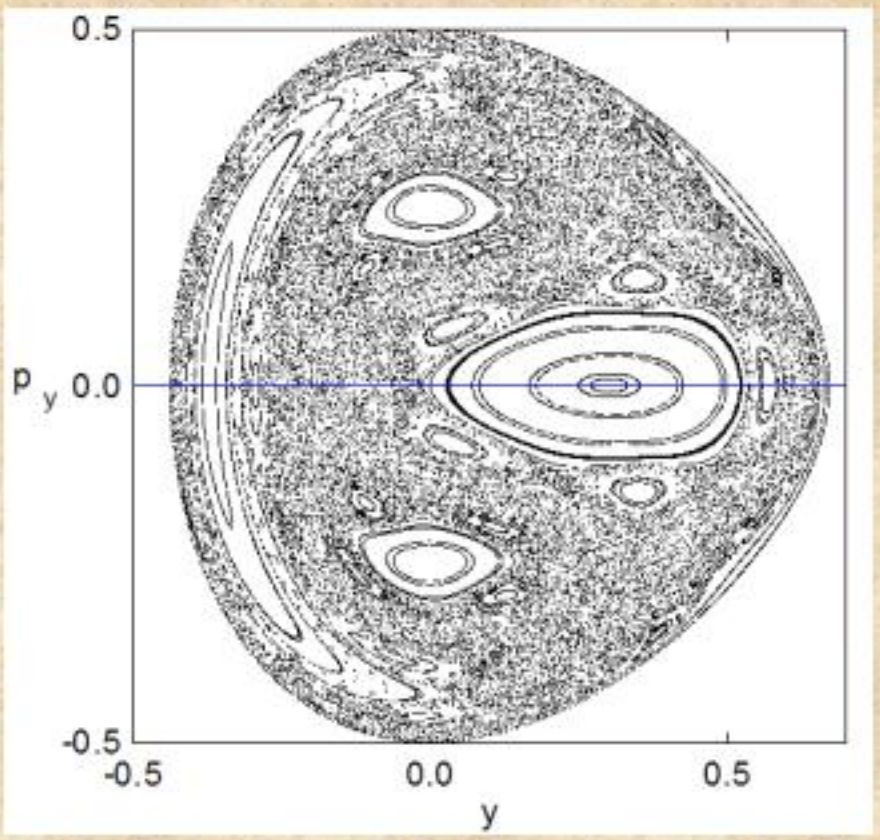

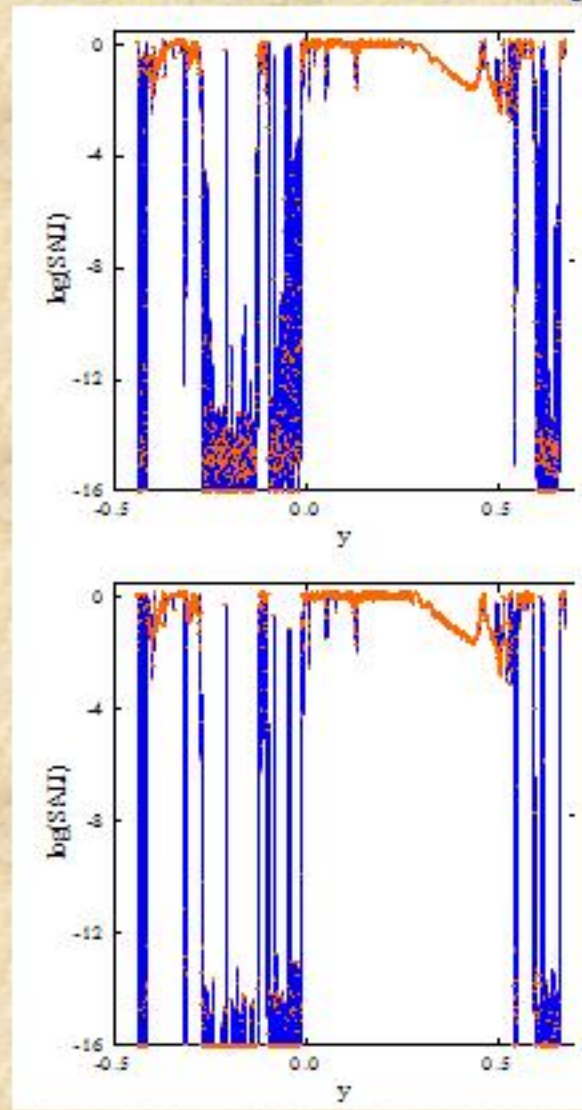

Applications – Hénon-Heiles system

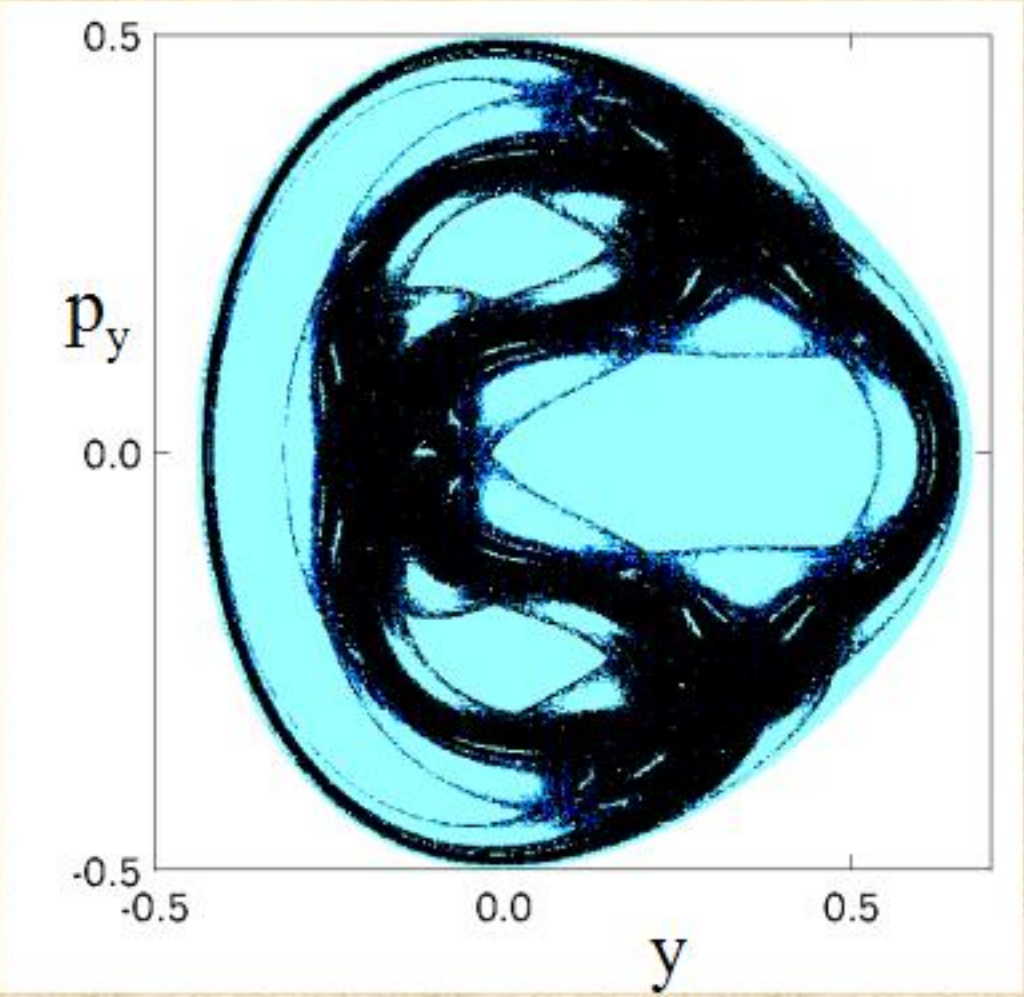

log(SALI) ≤ -12
-12 < log(SALI) ≤ -8
-8 < log(SALI) ≤ -4
-4 < log(SALI)

Applications – Hénon-Heiles system

The percentage of non chaotic orbits (SALI > 10^{-8} for t=1000)

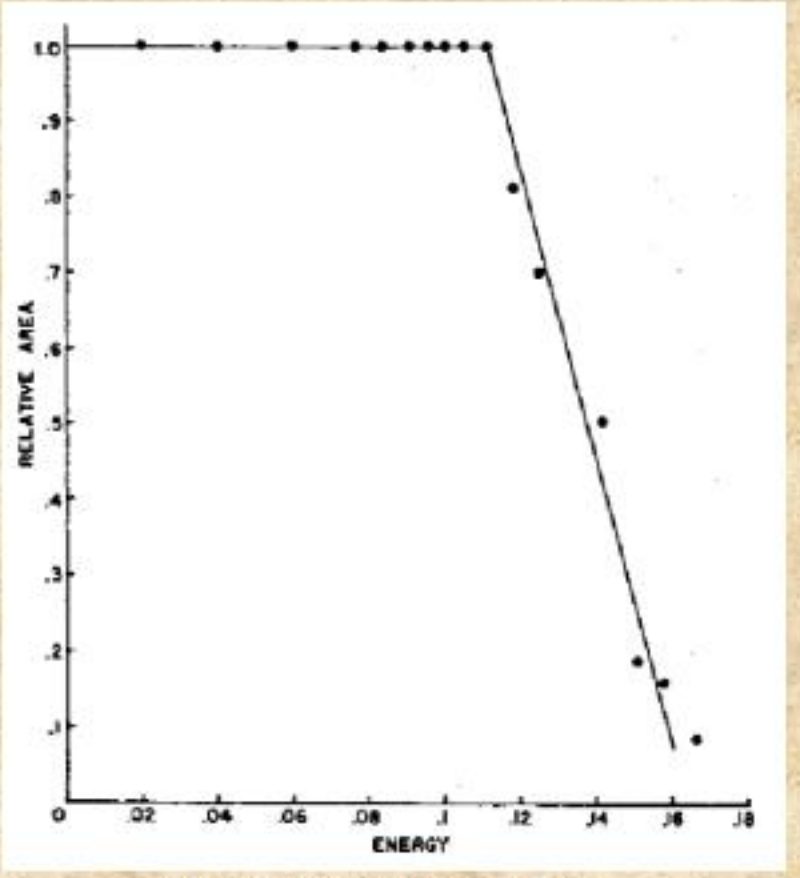

Hénon-Heiles (1964) Astron. J. 69, 73.

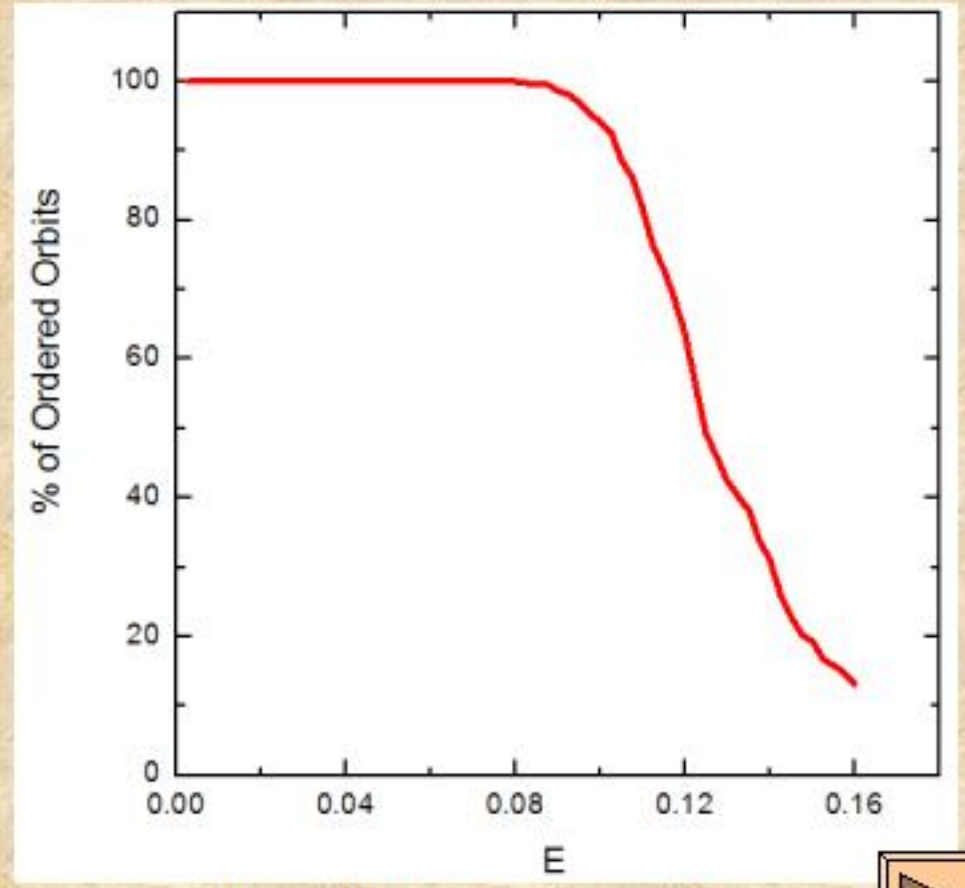

A. Manos (2004) Master Thesis, Univ. of Patras

Applications – 3D Hamiltonian

We consider the 3D Hamiltonian

$$H = \frac{1}{2}(p_x^2 + p_y^2 + p_z^2) + \frac{1}{2}(Ax^2 + By^2 + Cz^2) - \varepsilon xz^2 - \eta yz^2$$

with A=0.9, B=0.4, C=0.225, ε=0.56, η=0.2, H=0.00765.

Behavior of the SALI for ordered and chaotic orbits

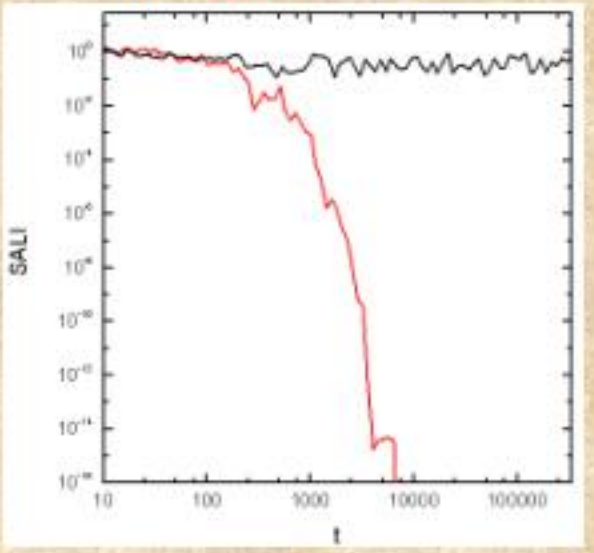

Color plot of the subspace $y=z=p_y=0$, $p_z>0$

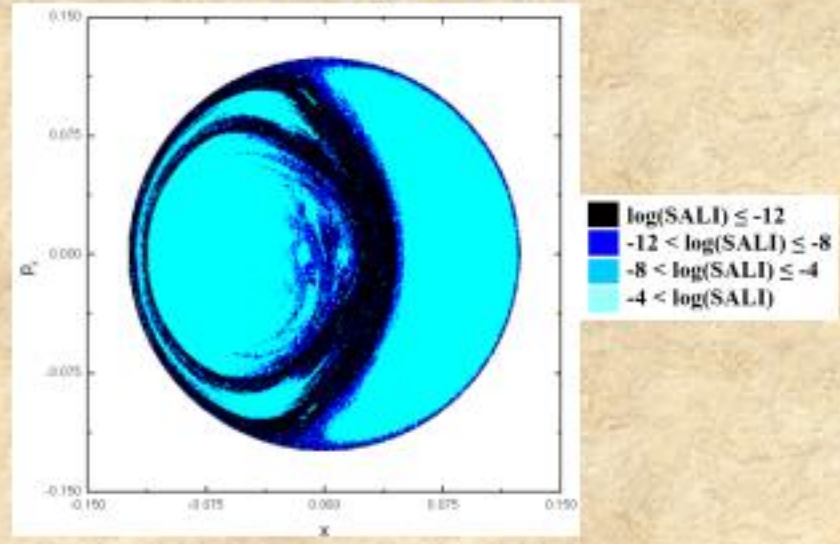

Applications – 4D map

$$
\begin{aligned}
x_1' &= x_1 + x_2 \\
x_2' &= x_2 - \nu \sin(x_1 + x_2) - \mu\,[1 - \cos(x_1 + x_2 + x_3 + x_4)] \\
x_3' &= x_3 + x_4 \\
x_4' &= x_4 - \kappa \sin(x_3 + x_4) - \mu\,[1 - \cos(x_1 + x_2 + x_3 + x_4)]
\end{aligned}
\qquad (\mathrm{mod}\ 2\pi)
$$

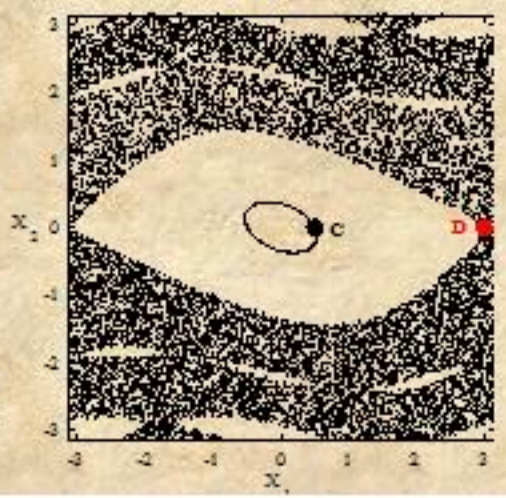

For ν=0.5, κ=0.1, μ=0.1 we consider the orbits:

ordered orbit C *with initial conditions* x_1=0.5, x_2=0, x_3=0.5, x_4=0.

chaotic orbit D *with initial conditions* x_1=3, x_2=0, x_3=0.5, x_4=0.

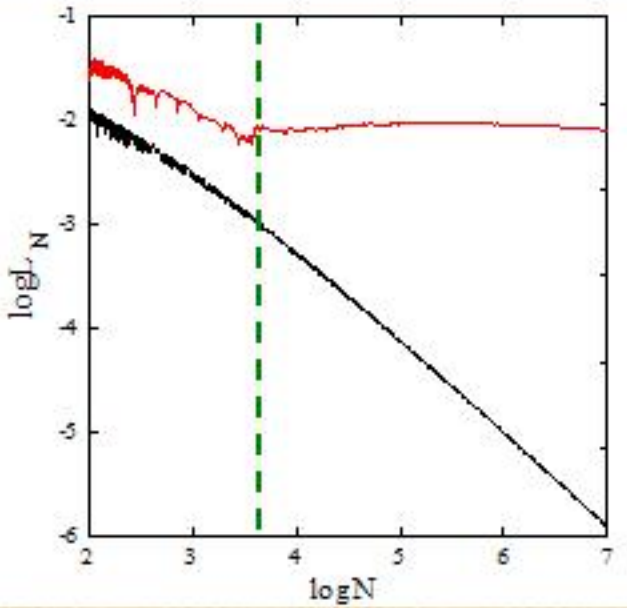

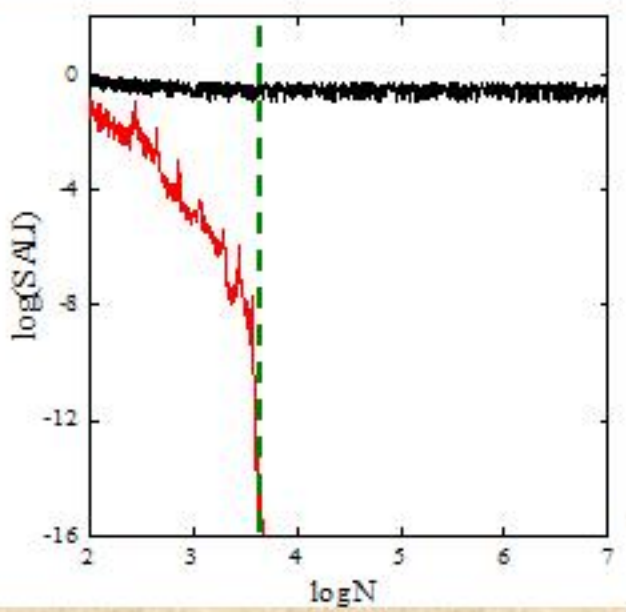

Applications – 4D Accelerator map

We consider the 4D symplectic map

$$\begin{pmatrix} x_1' \\ x_2' \\ x_3' \\ x_4' \end{pmatrix} = \begin{pmatrix} \cos\omega_1 & -\sin\omega_1 & 0 & 0 \\ \sin\omega_1 & \cos\omega_1 & 0 & 0 \\ 0 & 0 & \cos\omega_2 & -\sin\omega_2 \\ 0 & 0 & \sin\omega_2 & \cos\omega_2 \end{pmatrix} \times \begin{pmatrix} x_1 \\ x_2 + x_1^2 - x_3^2 \\ x_3 \\ x_4 - 2x_1x_3 \end{pmatrix}$$

describing the instantaneous sextupole 'kicks' experienced by a particle as it passes through an accelerator (Turchetti & Scandale 1991, Bountis & Tompaidis 1991, Vrahatis et al. 1996, 1997).

x_1 and x_3 are the particle's deflections from the ideal circular orbit, in the horizontal and vertical directions respectively.

x_2 and x_4 are the associated momenta

ω_1, ω_2 are related to the accelerator's tunes q_x, q_y by

$$\omega_1 = 2\pi q_x, \quad \omega_2 = 2\pi q_y$$

Our problem is to estimate the region of stability of the particle's motion, the so-called dynamic aperture of the beam (Bountis & Skokos, 2006, Nucl. Inst Meth. Phys Res. A).

4D Accelerator map – "Global" study

Regions of different values of the SALI on the subspace $x_2(0)=x_4(0)=0$, after 10^4 iterations ($q_x=0.61803$ $q_y=0.4152$)

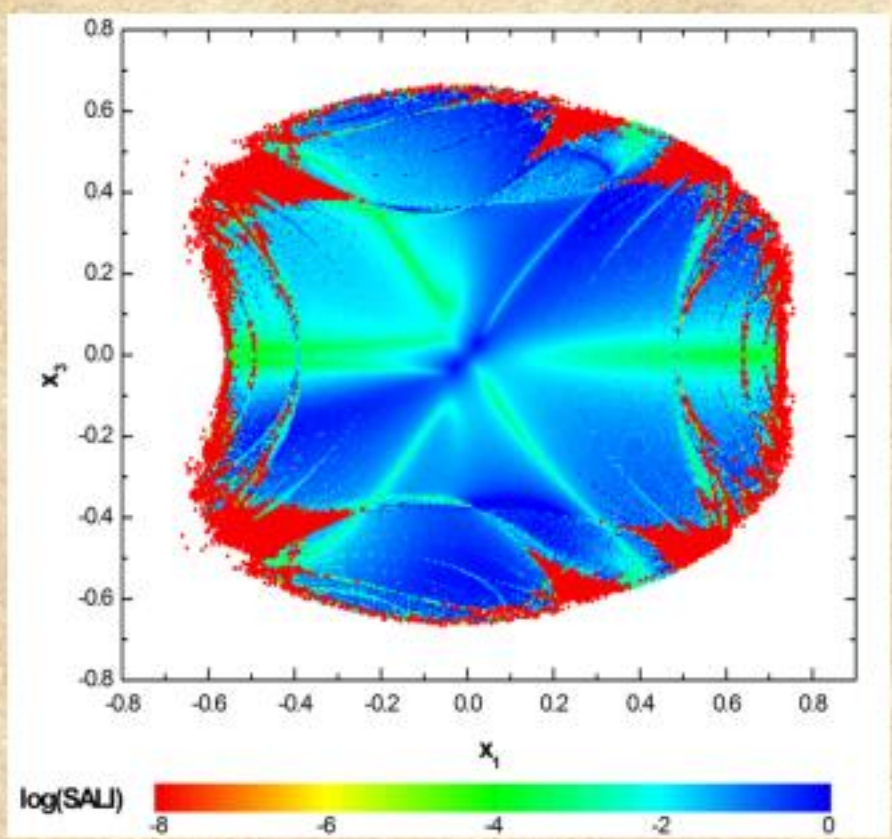

4D Accelerator map – "Global" study

We consider 1,922,833 orbits by varying all x_1, x_2, x_3, x_4 within spherical shells of width 0.01 in a hypersphere of radius 1. (q_x=0.61803 q_y=0.4152)

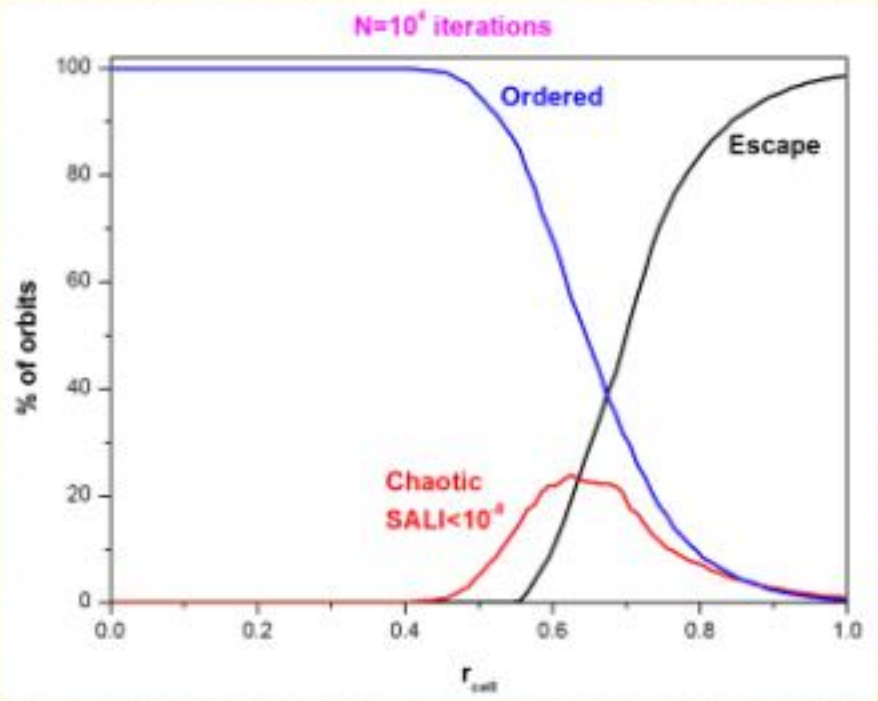

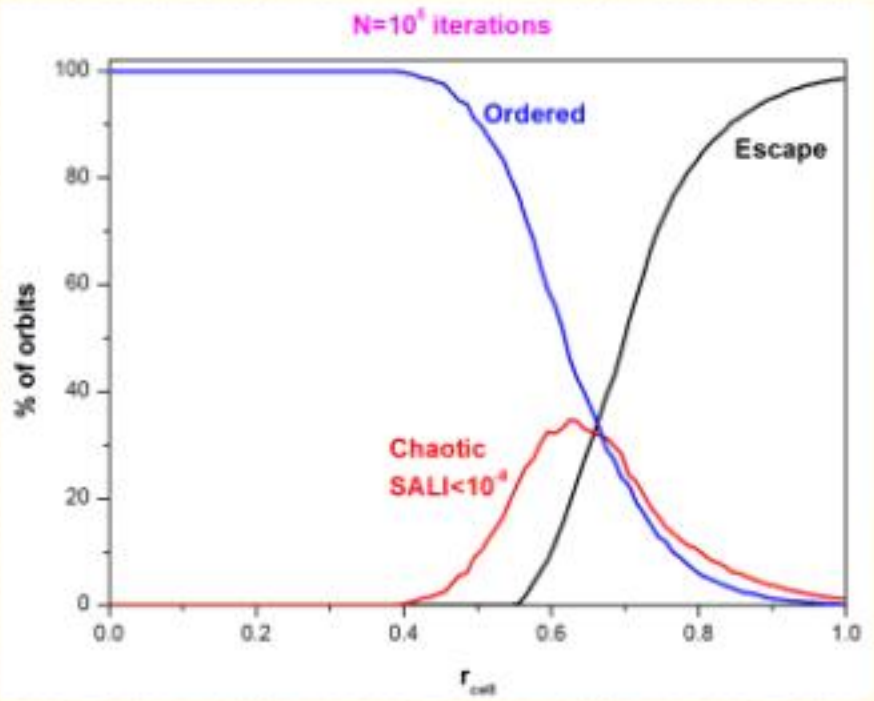

Applications – 2D map

$$x_1' = x_1 + x_2$$
$$x_2' = x_2 - \nu \sin(x_1 + x_2) \qquad (\mathrm{mod}\ 2\pi)$$

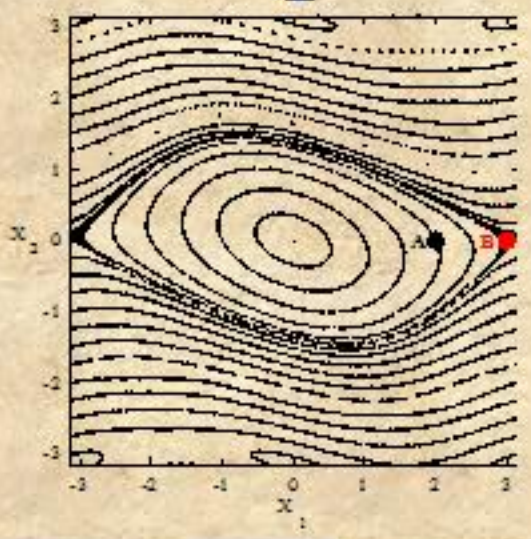

For ν=0.5 we consider the orbits:
ordered orbit A *with initial conditions* $x_1=2$, $x_2=0$.
chaotic orbit B *with initial conditions* $x_1=3$, $x_2=0$.

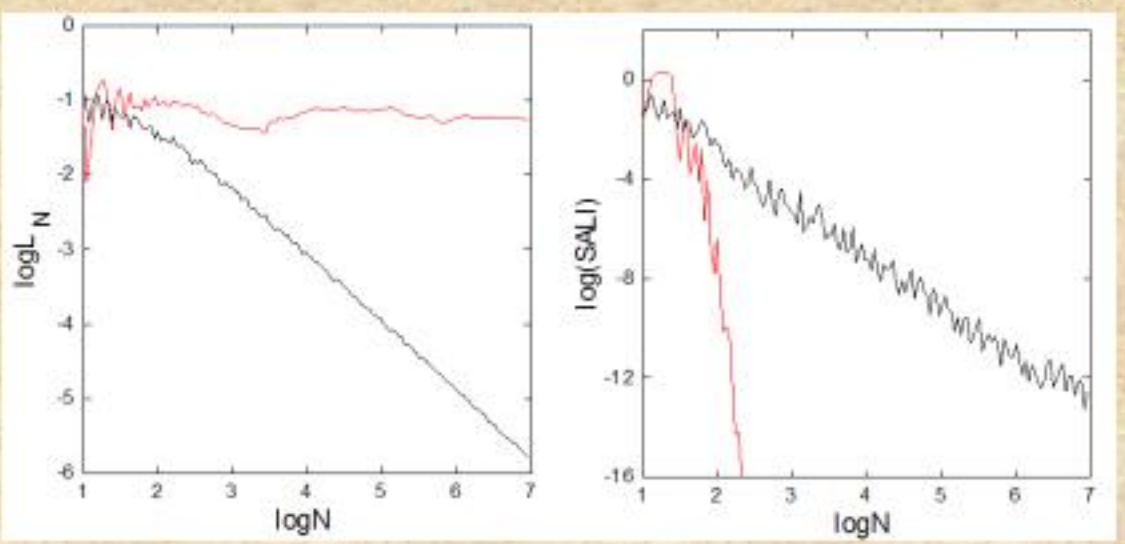

Applications – Standard map

K=2

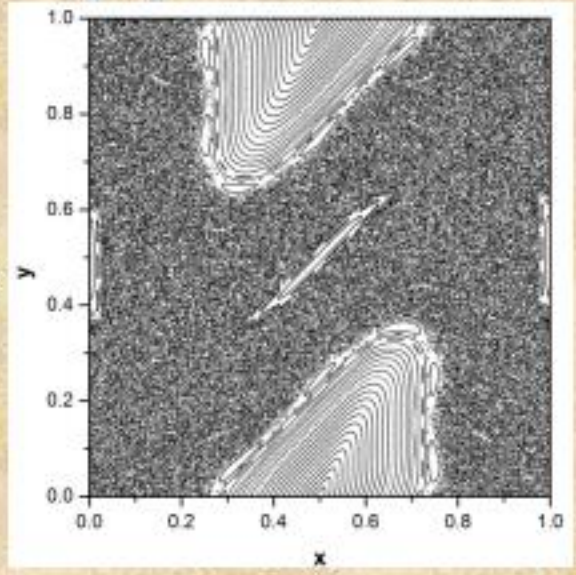

$$x' = x + y' \qquad \text{(mod 1)}$$

$$y' = y + \frac{K}{2\pi}\sin(2\pi x)$$

Dependence of the percentage of regular motion on K (Dvorak et al. 2003).

For every K (dK=0.001) we use a 1000 X 1000 grid of initial conditions. N=500.

Chaotic orbits: SALI<10^{-10}

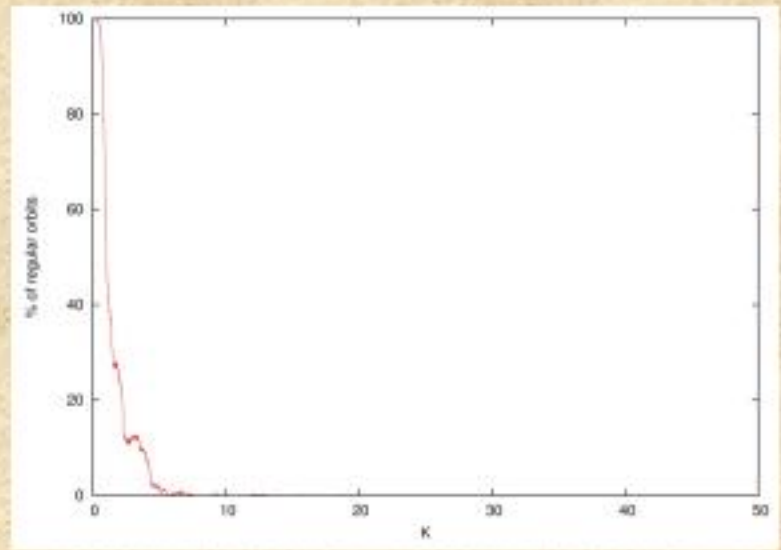

Applications – Standard map

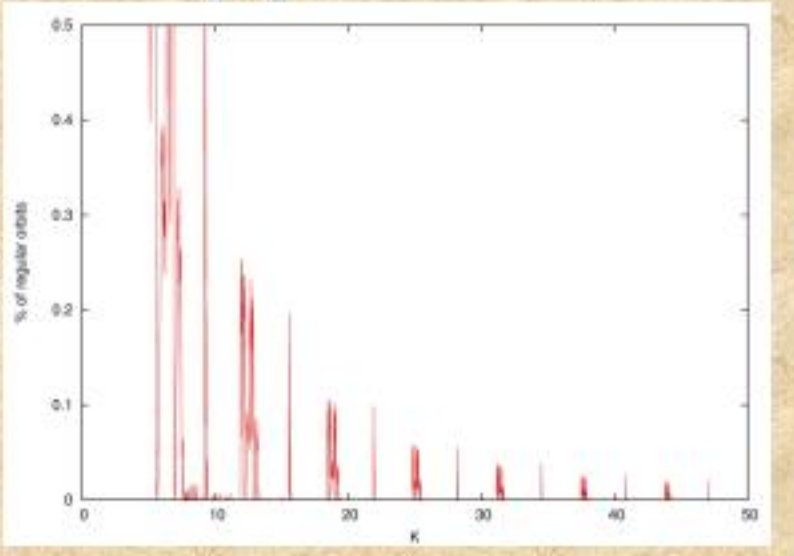

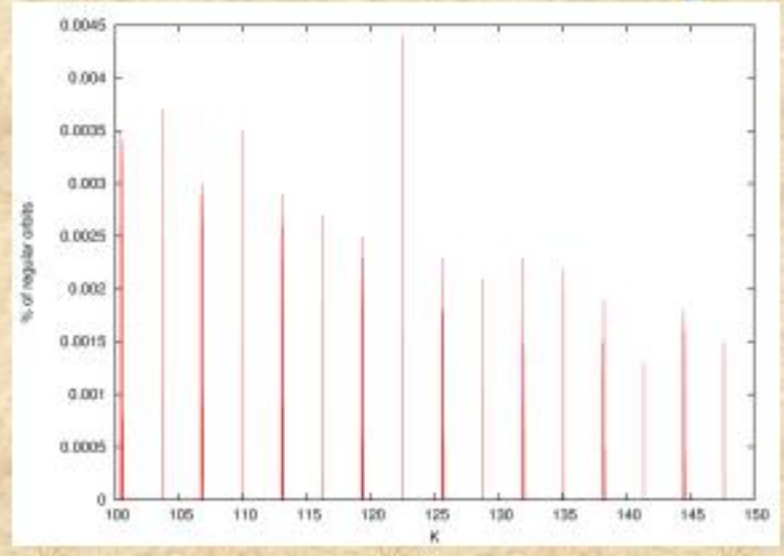

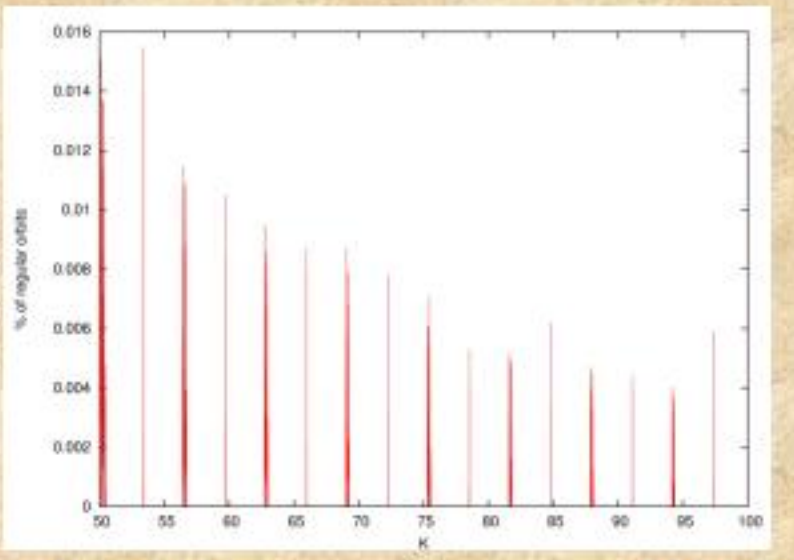

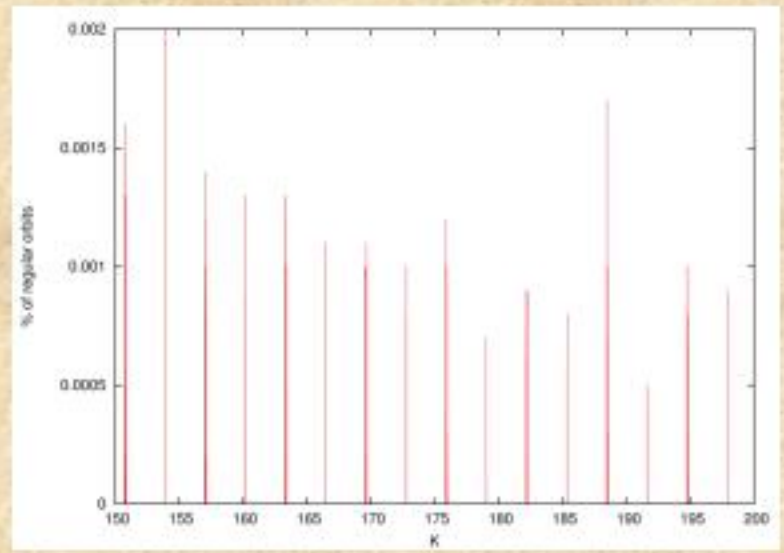

Applications – Standard map

For K=194.793 we have only 0.0004% regular orbits.

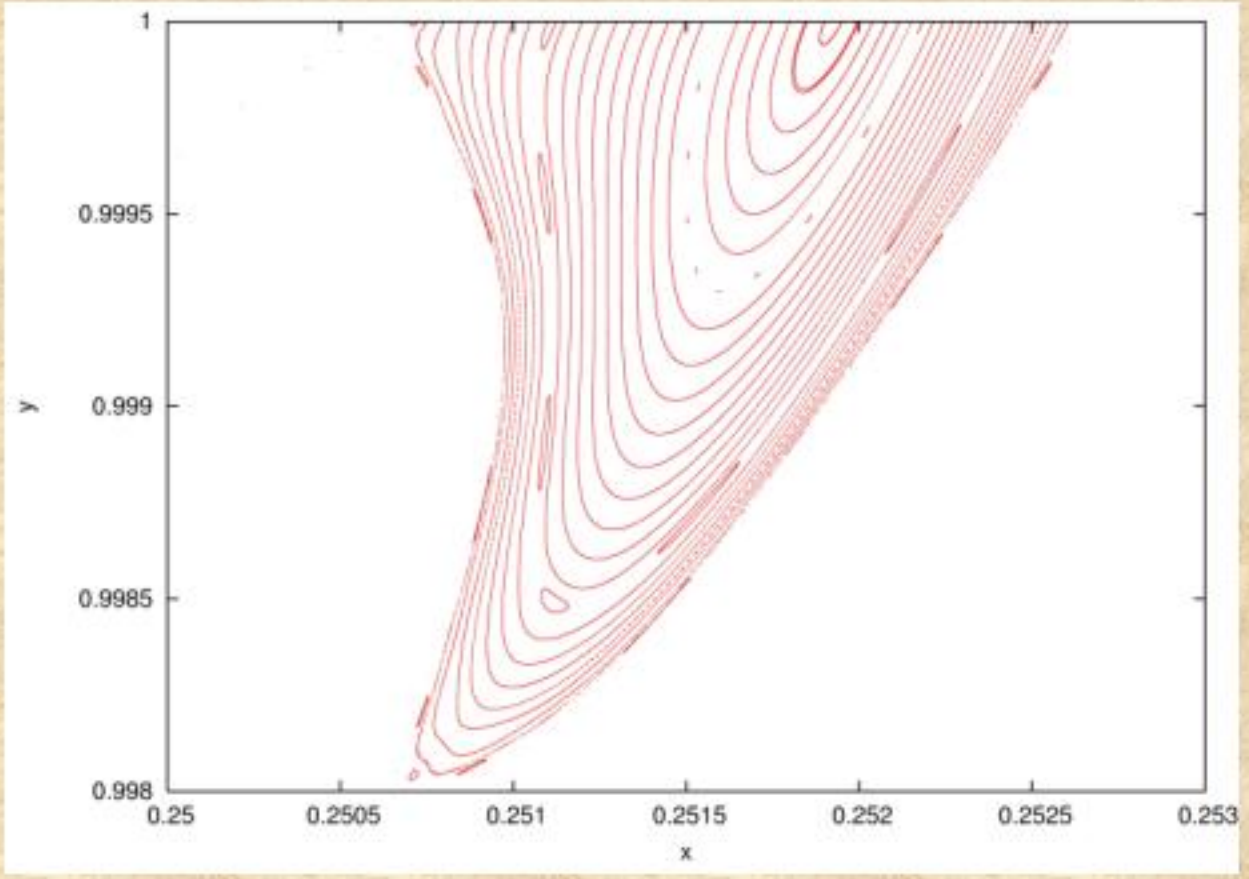

Behavior of SALI

2D maps

SALI→0 both for regular and chaotic orbits

following, however, completely different time rates which allows us to distinguish between the two cases.

Hamiltonian flows and multidimensional maps

SALI→0 for chaotic orbits

SALI→constant ≠ 0 for regular orbits

Questions

Can we generalize SALI so that the new index:

- **Can rapidly reveal the nature of chaotic orbits with $\sigma_1 \approx \sigma_2$ ($SALI \propto e^{-(\sigma 1 - \sigma 2)t}$)?**

- **Depends on several Lyapunov exponents for chaotic orbits?**

- **Exhibits power-law decay for regular orbits depending on the dimensionality of the tangent space of the reference orbit as for 2D maps?**

The Generalized ALignment Indices (GALIs) method

Definition of Generalized Alignment Index (GALI)

SALI effectively measures the 'area' of the parallelogram formed by the two deviation vectors.

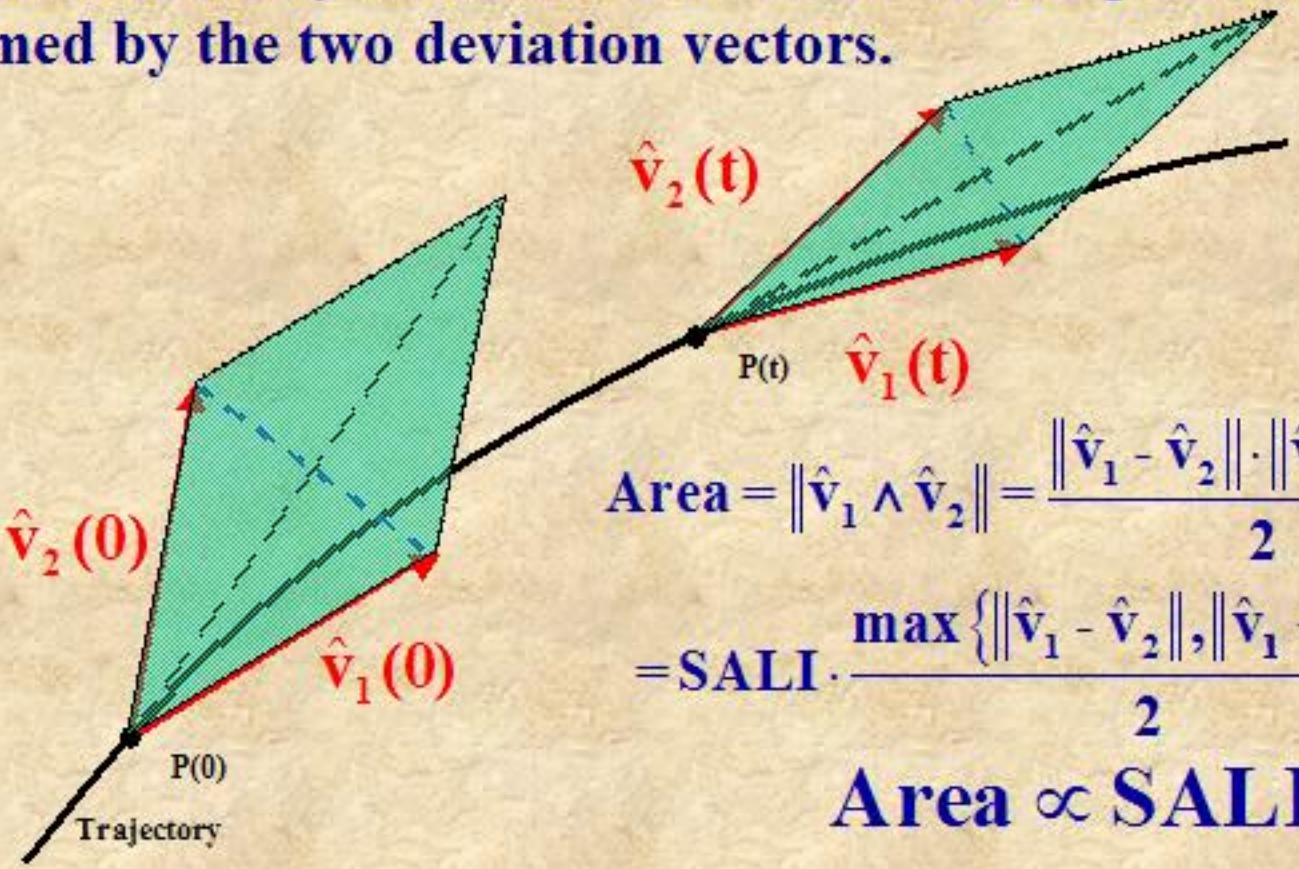

$$\text{Area} = \|\hat{v}_1 \wedge \hat{v}_2\| = \frac{\|\hat{v}_1 - \hat{v}_2\| \cdot \|\hat{v}_1 + \hat{v}_2\|}{2} =$$

$$= \text{SALI} \cdot \frac{\max\{\|\hat{v}_1 - \hat{v}_2\|, \|\hat{v}_1 + \hat{v}_2\|\}}{2} \Rightarrow$$

$$\text{Area} \propto \text{SALI}$$

Definition of GALI

Generalizing this idea to an N degree of freedom Hamiltonian system (Skokos et al., 2006, submitted), we follow the evolution of

k deviation vectors with $2 \leq k \leq 2N$,

and

define the Generalized Alignment Index (GALI) of order k :

$$GALI_k(t) = \left\| \hat{v}_1(t) \wedge \hat{v}_2(t) \wedge \ldots \wedge \hat{v}_k(t) \right\|$$

Clearly:

$$GALI_2(t) \propto SALI(t)$$

Computation of wedge product

We consider as a basis of the 2N-dimensional tangent space of the Hamiltonian flow the usual set of orthonormal vectors:

$$\hat{e}_1 = (1,0,0,...,0),\ \hat{e}_2 = (0,1,0,...,0),\ ...,\ \hat{e}_{2N} = (0,0,0,...,1)$$

Then for k deviation vectors we have:

$$\begin{bmatrix} \hat{v}_1 \\ \hat{v}_2 \\ \vdots \\ \hat{v}_k \end{bmatrix} = \begin{bmatrix} v_{11} & v_{12} & \cdots & v_{12N} \\ v_{21} & v_{22} & \cdots & v_{22N} \\ \vdots & \vdots & & \vdots \\ v_{k1} & v_{k2} & \cdots & v_{k2N} \end{bmatrix} \cdot \begin{bmatrix} \hat{e}_1 \\ \hat{e}_2 \\ \vdots \\ \hat{e}_{2N} \end{bmatrix}$$

$$\hat{v}_1 \wedge \hat{v}_2 \wedge \cdots \wedge \hat{v}_k = \sum_{1 \le i_1 < i_2 < \cdots < i_k \le 2N} \begin{vmatrix} v_{1 i_1} & v_{1 i_2} & \cdots & v_{1 i_k} \\ v_{2 i_1} & v_{2 i_2} & \cdots & v_{2 i_k} \\ \vdots & \vdots & & \vdots \\ v_{k i_1} & v_{k i_2} & \cdots & v_{k i_k} \end{vmatrix} \hat{e}_{i_1} \wedge \hat{e}_{i_2} \wedge \cdots \wedge \hat{e}_{i_k}$$

Computation of wedge product

We define as 'norm' of the wedge product the quantity :

$$\left\|\hat{\mathbf{v}}_1 \wedge \hat{\mathbf{v}}_2 \wedge \cdots \wedge \hat{\mathbf{v}}_k\right\| = \left\{ \sum_{1 \le i_1 < i_2 < \cdots < i_k \le 2N} \begin{vmatrix} v_{1 i_1} & v_{1 i_2} & \cdots & v_{1 i_k} \\ v_{2 i_1} & v_{2 i_2} & \cdots & v_{2 i_k} \\ \vdots & \vdots & & \vdots \\ v_{k i_1} & v_{k i_2} & \cdots & v_{k i_k} \end{vmatrix}^2 \right\}^{1/2}$$

Computation of GALI - Example

Let us compute $GALI_3$ in the case of 2D Hamiltonian system (4-dimensional phase space).

$$\begin{bmatrix} \hat{v}_1 \\ \hat{v}_2 \\ \hat{v}_3 \end{bmatrix} = \begin{bmatrix} v_{11} & v_{12} & v_{13} & v_{14} \\ v_{21} & v_{22} & v_{23} & v_{24} \\ v_{31} & v_{32} & v_{33} & v_{34} \end{bmatrix} \cdot \begin{bmatrix} \hat{e}_1 \\ \hat{e}_2 \\ \hat{e}_3 \\ \hat{e}_4 \end{bmatrix}$$

Columns 1 2 3 1 2 4

$$GALI_3 = \left\| \hat{v}_1 \wedge \hat{v}_2 \wedge \hat{v}_3 \right\| = \left\{ \begin{vmatrix} v_{11} & v_{12} & v_{13} \\ v_{21} & v_{22} & v_{23} \\ v_{31} & v_{32} & v_{33} \end{vmatrix}^2 + \begin{vmatrix} v_{11} & v_{12} & v_{14} \\ v_{21} & v_{22} & v_{24} \\ v_{31} & v_{32} & v_{34} \end{vmatrix}^2 + \right.$$

$$\left. \begin{vmatrix} v_{11} & v_{13} & v_{14} \\ v_{21} & v_{23} & v_{24} \\ v_{31} & v_{33} & v_{34} \end{vmatrix}^2 + \begin{vmatrix} v_{12} & v_{13} & v_{14} \\ v_{22} & v_{23} & v_{24} \\ v_{32} & v_{33} & v_{34} \end{vmatrix}^2 \right\}^{1/2}$$

1 3 4 2 3 4

Behavior of $GALI_k$ for chaotic motion

$GALI_k$ $(2 \leq k \leq 2N)$ tends exponentially to zero with exponents that involve the values of the first k largest Lyapunov exponents $\sigma_1, \sigma_2, \ldots, \sigma_k$ (Skokos et al., 2006, submitted) :

$$GALI_k(t) \propto e^{-[(\sigma_1-\sigma_2)+(\sigma_1-\sigma_3)+\ldots+(\sigma_1-\sigma_k)]t}$$

The above relation is valid even if some Lyapunov exponents are equal, or very close to each other.

Behavior of $GALI_k$ for chaotic motion

Using the approximation:

$$\mathbf{v}_i(t) = \sum_{j=1}^{2N} c_j^i e^{\sigma_j t}\hat{u}_j = c_1^i e^{\sigma_1 t}\hat{u}_1 + c_2^i e^{\sigma_2 t}\hat{u}_2 + \cdots + c_{2N}^i e^{\sigma_{2N} t}\hat{u}_{2N}, \qquad \|\mathbf{v}_i(t)\| \approx \left|c_1^i\right| e^{\sigma_1 t}$$

where $\sigma_1 \geq \sigma_2 \geq \ldots \geq \sigma_n$ are the Lyapunov exponents, and $\hat{u}_j$ j=1, 2, …, 2N the corresponding eigendirections, we get

$$\begin{bmatrix} \hat{v}_1 \\ \hat{v}_2 \\ \vdots \\ \hat{v}_k \end{bmatrix} = \begin{bmatrix} s_1 & \frac{c_2^1}{|c_1^1|} e^{-(\sigma_1-\sigma_2)t} & \frac{c_3^1}{|c_1^1|} e^{-(\sigma_1-\sigma_3)t} & \cdots & \frac{c_{2N}^1}{|c_1^1|} e^{-(\sigma_1-\sigma_{2N})t} \\ s_2 & \frac{c_2^2}{|c_1^2|} e^{-(\sigma_1-\sigma_2)t} & \frac{c_3^2}{|c_1^2|} e^{-(\sigma_1-\sigma_3)t} & \cdots & \frac{c_{2N}^2}{|c_1^2|} e^{-(\sigma_1-\sigma_{2N})t} \\ \vdots & \vdots & \vdots & & \vdots \\ s_k & \frac{c_2^k}{|c_1^k|} e^{-(\sigma_1-\sigma_2)t} & \frac{c_3^k}{|c_1^k|} e^{-(\sigma_1-\sigma_3)t} & \cdots & \frac{c_{2N}^k}{|c_1^k|} e^{-(\sigma_1-\sigma_{2N})t} \end{bmatrix} \cdot \begin{bmatrix} \hat{u}_1 \\ \hat{u}_2 \\ \vdots \\ \hat{u}_{2N} \end{bmatrix}$$

with $s_i = \mathrm{sign}(c_1^i)$.

Behavior of $GALI_k$ for chaotic motion

From all determinants appearing in the definition of $GALI_k$ the one that decreases the slowest is the one containing the first k columns of the previous matrix:

$$\begin{vmatrix} s_1 & \frac{c_2^1}{|c_1^1|} e^{-(\sigma_1-\sigma_2)t} & \frac{c_3^1}{|c_1^1|} e^{-(\sigma_1-\sigma_3)t} & \cdots & \frac{c_k^1}{|c_1^1|} e^{-(\sigma_1-\sigma_k)t} \\ s_2 & \frac{c_2^2}{|c_1^2|} e^{-(\sigma_1-\sigma_2)t} & \frac{c_3^2}{|c_1^2|} e^{-(\sigma_1-\sigma_3)t} & \cdots & \frac{c_k^2}{|c_1^2|} e^{-(\sigma_1-\sigma_k)t} \\ \vdots & \vdots & \vdots & & \vdots \\ s_k & \frac{c_2^k}{|c_1^k|} e^{-(\sigma_1-\sigma_2)t} & \frac{c_3^k}{|c_1^k|} e^{-(\sigma_1-\sigma_3)t} & \cdots & \frac{c_k^k}{|c_1^k|} e^{-(\sigma_1-\sigma_k)t} \end{vmatrix} = \begin{vmatrix} s_1 & \frac{c_2^1}{|c_1^1|} & \frac{c_3^1}{|c_1^1|} & \cdots & \frac{c_k^1}{|c_1^1|} \\ s_2 & \frac{c_2^2}{|c_1^2|} & \frac{c_3^2}{|c_1^2|} & \cdots & \frac{c_k^2}{|c_1^2|} \\ \vdots & \vdots & \vdots & & \vdots \\ s_k & \frac{c_2^k}{|c_1^k|} & \frac{c_3^k}{|c_1^k|} & \cdots & \frac{c_k^k}{|c_1^k|} \end{vmatrix} \cdot e^{-[(\sigma_1-\sigma_2)+(\sigma_1-\sigma_3)+\cdots+(\sigma_1-\sigma_k)]t}$$

Thus

$$GALI_k(t) \propto e^{-[(\sigma_1-\sigma_2)+(\sigma_1-\sigma_3)+\ldots+(\sigma_1-\sigma_k)]t}$$

Behavior of $GALI_k$ for chaotic motion

2D Hamiltonian (Hénon-Heiles system)

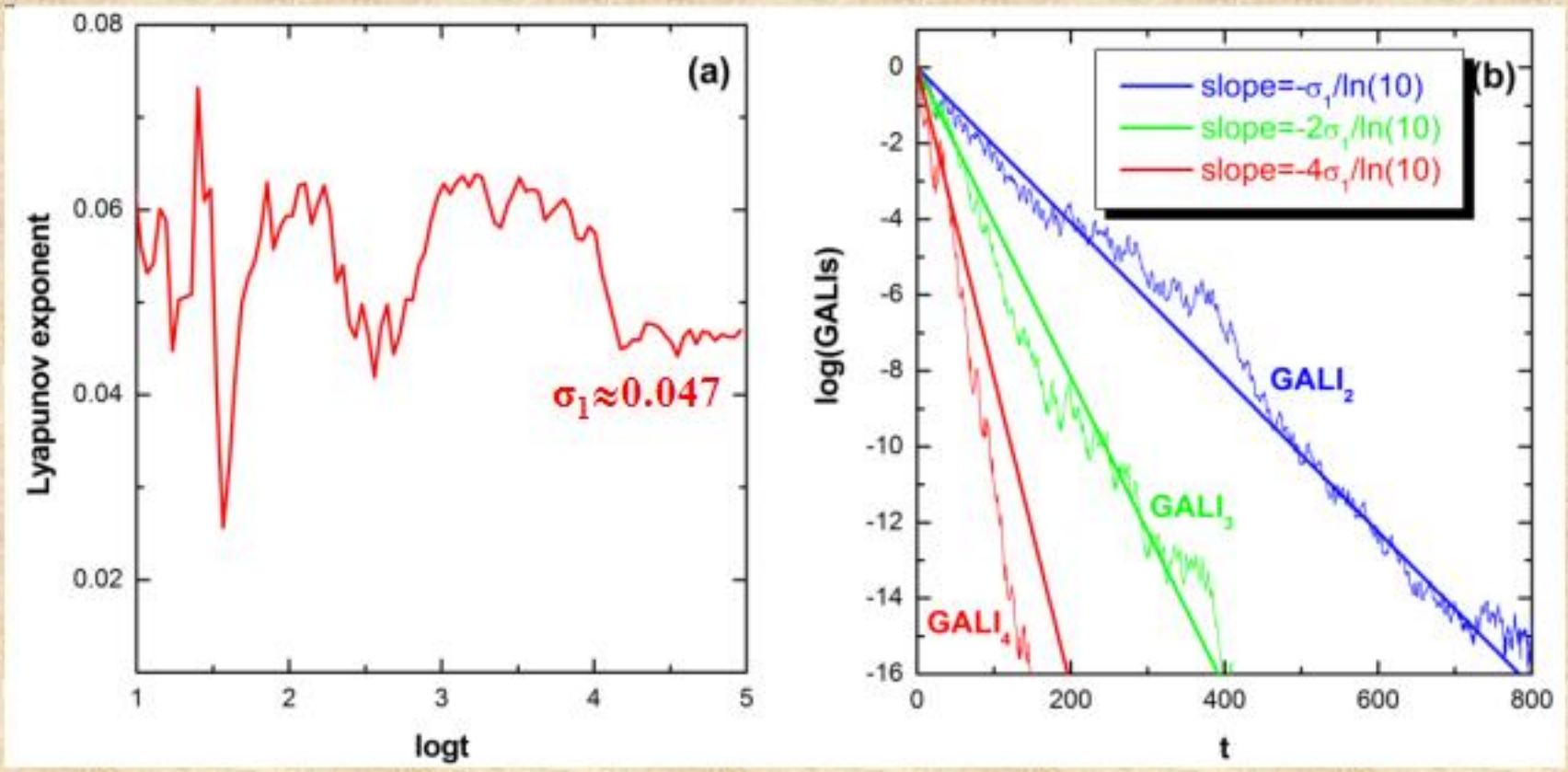

Behavior of $GALI_k$ for chaotic motion

3D system:

$$H_3 = \sum_{i=1}^{3} \frac{\omega_i}{2}(q_i^2 + p_i^2) + q_1^2 q_2 + q_1^2 q_3$$

with $\omega_1=1$, $\omega_2=\sqrt{2}$, $\omega_3=\sqrt{3}$, $H_3=0.09$.

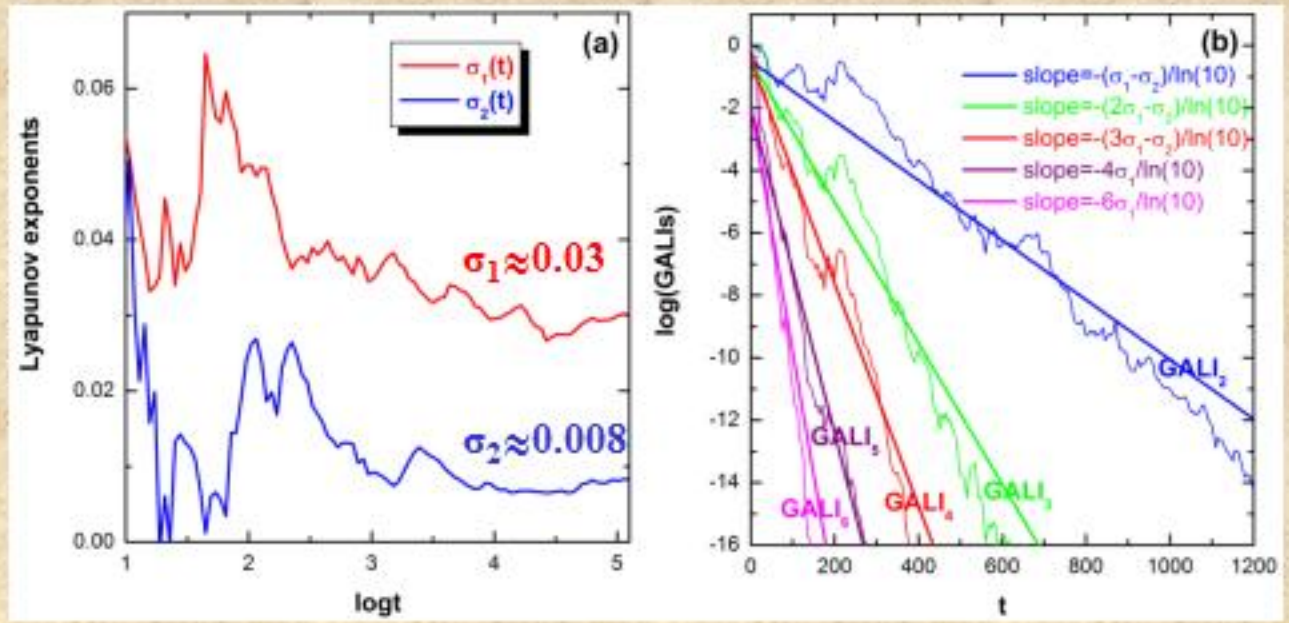

Behavior of $GALI_k$ for chaotic motion

15D Fermi-Pasta-Ulam (FPU) system:

$$H_{15} = \frac{1}{2}\sum_{i=1}^{15} p_i^2 + \sum_{i=1}^{15}\left[\frac{1}{2}(q_{i+1}-q_i)^2 + \frac{1}{4}\beta(q_{i+1}-q_i)^4\right]$$

with H_{15}=26.68777 and β=1.04.

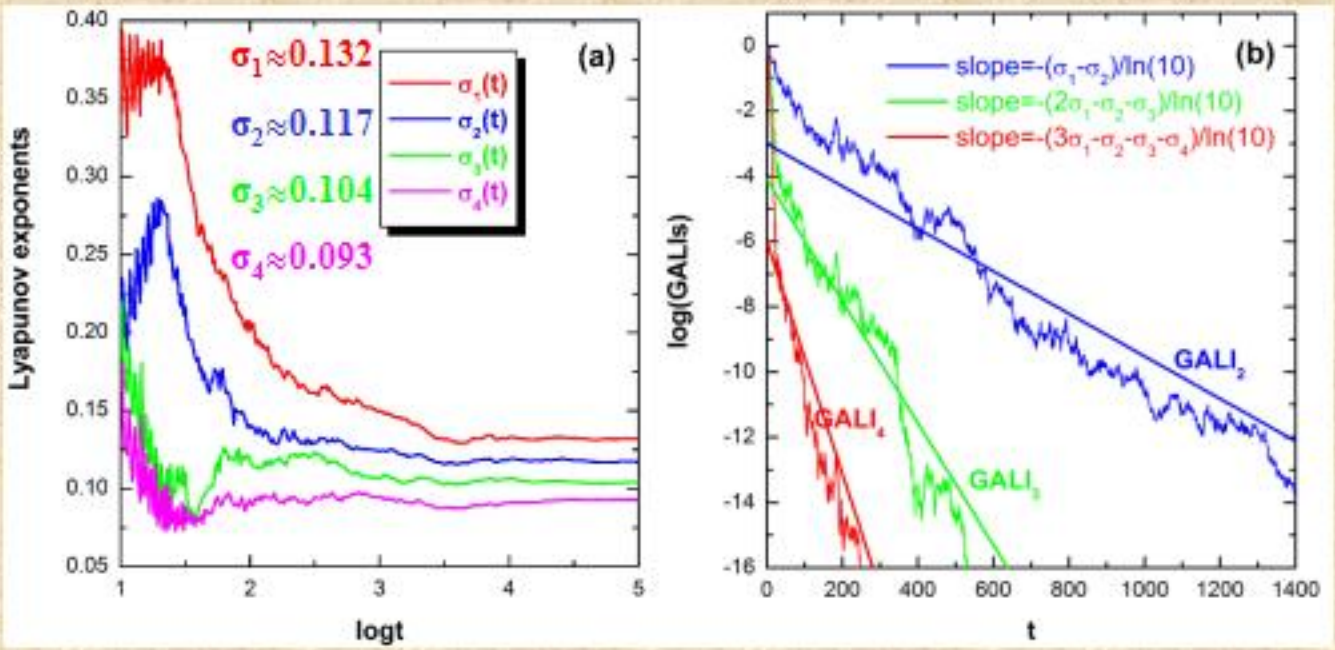

Behavior of $GALI_k$ for chaotic motion

15D Hamiltonian – close to an unstable periodic orbit

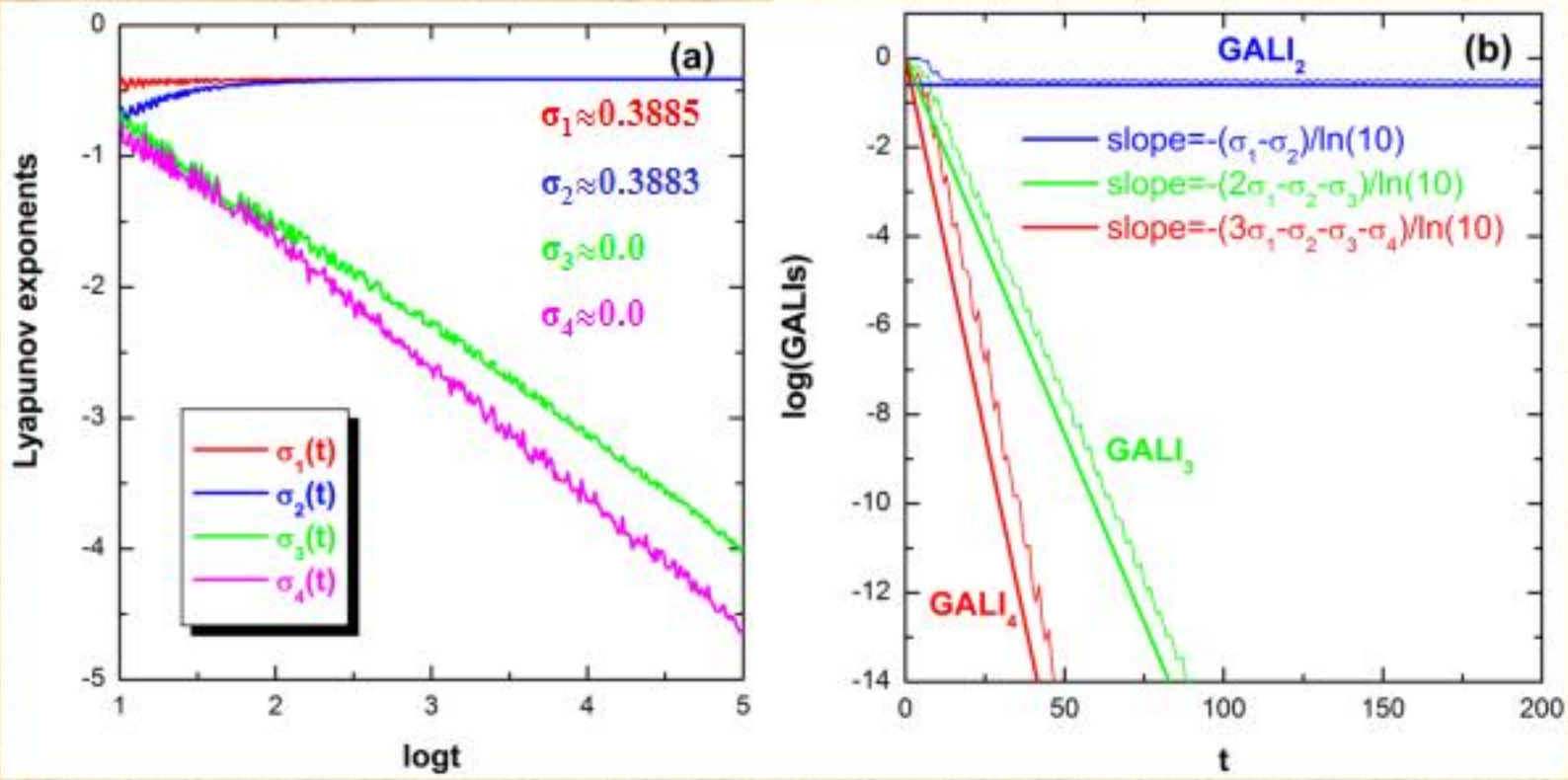

Behavior of $GALI_k$ for regular motion

$GALI_k$ remains essentially constant when $2 \le k \le N$, while it tends to zero for $N < k \le 2N$ following a power law, which depends on the number m ($m \le N$ and $m \le k$) of deviation vectors that are initially tangent to the torus on which the motion lies:

$$GALI_k(t) \propto \begin{cases} \text{constant} & \text{if} \quad 2 \le k \le N \\ \dfrac{1}{t^{2(k-N)-m}} & \text{if} \quad N < k \le 2N \text{ and } 0 \le m < k-N \\ \dfrac{1}{t^{k-N}} & \text{if} \quad N < k \le 2N \text{ and } m \ge k-N \end{cases}$$

Behavior of $GALI_k$ for regular motion

Regular orbits of an N degree of freedom Hamiltonian system lie on N-dimensional tori.

Performing a local transformation to action-angle variables we get for the Hamilton's equations of motion:

$$\left.\begin{aligned} \dot{J}_i &= 0 \\ \dot{\theta}_i &= \omega_i(J_1, J_2, \ldots, J_N) \end{aligned}\right\} \Rightarrow \begin{aligned} J_i(t) &= J_{i0} \\ \theta_i(t) &= \theta_{i0} + \omega_i(J_{10}, J_{20}, \ldots, J_{N0}) \cdot t \end{aligned}, \quad i = 1, 2, \ldots, N$$

where J_{i0}, θ_{i0}, i=1,2,…,N are the initial conditions.

Behavior of $GALI_k$ for regular motion

The variational equations give:

$$\left.\begin{aligned} \dot{\xi}_i &= 0 \\ \dot{\eta}_i &= \sum_{j=1}^{N} \omega_{ij} \cdot \xi_j \end{aligned}\right\} \Rightarrow \begin{aligned} \xi_i(t) &= \xi_i(0) \\ \eta_i(t) &= \eta_i(0) + \left[\sum_{j=1}^{N} \omega_{ij} \cdot \xi_j(0)\right] \cdot t \end{aligned}, \quad i = 1,2,\ldots,N$$

where $\omega_{ij}=\partial\omega_i/\partial J_j|_{J0}$, i=1,2,…,N are constants.

Using as a basis of the 2N-dimensional tangent space of the flow the 2N unit vectors $\{\hat{u}_1,\hat{u}_2,...,\hat{u}_{2N}\}$ such that the first N of them, $\hat{u}_1,\hat{u}_2,...,\hat{u}_N$ correspond to the N action variables and the N remaining ones, $\hat{u}_{N+1},\hat{u}_{N+2},...,\hat{u}_{2N}$ to the conjugate angle variables, we write any unit deviation vector as:

$$\hat{v}_i(t) = \frac{1}{\|v_i(t)\|}\left[\sum_{j=1}^{N}\xi_j^i(0)\hat{u}_j + \sum_{j=1}^{N}\left(\eta_j^i(0) + \sum_{k=1}^{N}\omega_{kj}\xi_j^i(0)\,t\right)\hat{u}_{N+j}\right]$$

$$\text{with} \quad \|v_i(t)\| \propto t$$

Behavior of $GALI_k$ for regular motion

For k deviation vectors we have:

$$\begin{bmatrix} \hat{\mathbf{v}}_1 \\ \hat{\mathbf{v}}_2 \\ \vdots \\ \hat{\mathbf{v}}_k \end{bmatrix} = \frac{1}{\prod_{m=1}^{k} \|\mathbf{v}_m(t)\|} \cdot$$

$$\cdot \begin{bmatrix} \xi_1^1(0) & \cdots & \xi_N^1(0) & \eta_1^1(0) + \sum_{m=1}^{N} \omega_{1m} \xi_m^1(0)\, t & \cdots & \eta_N^1(0) + \sum_{m=1}^{N} \omega_{Nm} \xi_m^1(0)\, t \\ \xi_1^2(0) & \cdots & \xi_N^2(0) & \eta_1^2(0) + \sum_{m=1}^{N} \omega_{1m} \xi_m^2(0)\, t & \cdots & \eta_N^2(0) + \sum_{m=1}^{N} \omega_{Nm} \xi_m^2(0)\, t \\ \vdots & & \vdots & \vdots & & \vdots \\ \xi_1^k(0) & \cdots & \xi_N^k(0) & \eta_1^k(0) + \sum_{m=1}^{N} \omega_{1m} \xi_m^k(0)\, t & \cdots & \eta_N^k(0) + \sum_{m=1}^{N} \omega_{Nm} \xi_m^k(0)\, t \end{bmatrix} \cdot \begin{bmatrix} \hat{\mathbf{u}}_1 \\ \hat{\mathbf{u}}_2 \\ \vdots \\ \hat{\mathbf{u}}_{2N} \end{bmatrix}$$

Behavior of $GALI_k$ for regular motion

For $2 \le k \le N$ the slowest decreasing determinants are the ones whose k columns are chosen among the last N columns of the evolution matrix

$$\frac{1}{\prod_{m=1}^{k} \|v_m(t)\|} \cdot \begin{vmatrix} \eta^1_{j_1}(0) + \sum_{m=1}^{N} \omega_{j_1 m} \xi^1_m(0)\, t & \cdots & \eta^1_{j_k}(0) + \sum_{m=1}^{N} \omega_{j_k m} \xi^1_m(0)\, t \\ \eta^2_{j_1}(0) + \sum_{m=1}^{N} \omega_{j_1 m} \xi^2_m(0)\, t & \cdots & \eta^2_{j_k}(0) + \sum_{m=1}^{N} \omega_{j_k m} \xi^2_m(0)\, t \\ \vdots & & \vdots \\ \eta^k_{j_1}(0) + \sum_{m=1}^{N} \omega_{j_1 m} \xi^k_m(0)\, t & \cdots & \eta^2_{j_k}(0) + \sum_{m=1}^{N} \omega_{j_k m} \xi^k_m(0)\, t \end{vmatrix} \propto$$

$$\propto \frac{1}{t^k} \cdot \begin{vmatrix} \omega_{j_2 m_1} \xi^1_{m_1}(0)\, t & \cdots & \omega_{j_k m_k} \xi^1_{m_k}(0)\, t \\ \omega_{j_2 m_1} \xi^2_{m_1}(0)\, t & \cdots & \omega_{j_k m_k} \xi^2_{m_k}(0)\, t \\ \vdots & & \vdots \\ \omega_{j_2 m_1} \xi^k_{m_1}(0)\, t & \cdots & \omega_{j_k m_k} \xi^k_{m_k}(0)\, t \end{vmatrix} \propto \frac{1}{t^k} \cdot t^k \cdot \begin{vmatrix} \omega_{j_2 m_1} \xi^1_{m_1}(0) & \cdots & \omega_{j_k m_k} \xi^1_{m_k}(0) \\ \omega_{j_2 m_1} \xi^2_{m_1}(0) & \cdots & \omega_{j_k m_k} \xi^2_{m_k}(0) \\ \vdots & & \vdots \\ \omega_{j_2 m_1} \xi^k_{m_1}(0) & \cdots & \omega_{j_k m_k} \xi^k_{m_k}(0) \end{vmatrix} \approx \text{constant}$$

Behavior of $GALI_k$ for regular motion

For $N<k\leq 2N$ the slowest decreasing determinants are the ones containing the last N columns of the evolution matrix

$$\frac{1}{\prod_{m=1}^{k}\|v_m(t)\|}\cdot\begin{vmatrix} \xi^1_{j_1}(0) & \cdots & \xi^1_{j_{k-N}}(0) & \eta^1_1(0)+\sum_{m=1}^{N}\omega_{1m}\xi^1_m(0)\,t & \cdots & \eta^1_N(0)+\sum_{m=1}^{N}\omega_{Nm}\xi^1_m(0)\,t \\ \xi^2_{j_1}(0) & \cdots & \xi^2_{j_{k-N}}(0) & \eta^2_1(0)+\sum_{m=1}^{N}\omega_{1m}\xi^2_m(0)\,t & \cdots & \eta^2_N(0)+\sum_{m=1}^{N}\omega_{Nm}\xi^2_m(0)\,t \\ \vdots & & \vdots & \vdots & & \vdots \\ \xi^k_{j_1}(0) & \cdots & \xi^k_{j_{k-N}}(0) & \eta^k_1(0)+\sum_{m=1}^{N}\omega_{1m}\xi^k_m(0)\,t & \cdots & \eta^k_N(0)+\sum_{m=1}^{N}\omega_{Nm}\xi^k_m(0)\,t \end{vmatrix} \propto$$

k-N columns | k-N columns | 2N-k columns

$$\propto \frac{1}{t^k}\cdot\begin{vmatrix} \xi^1_{j_1}(0) & \cdots & \xi^1_{j_{k-N}}(0) & \eta^1_{i_1}(0) & \cdots & \eta^1_{i_{k-N}}(0) & \omega_{i_{k-N+1}m_1}\xi^1_{m_1}(0)\,t & \cdots & \omega_{i_Nm_{2N-k}}\xi^1_{m_1}(0)\,t \\ \xi^2_{j_1}(0) & \cdots & \xi^2_{j_{k-N}}(0) & \eta^2_{i_1}(0) & \cdots & \eta^2_{i_{k-N}}(0) & \omega_{i_{k-N+1}m_1}\xi^2_{m_1}(0)\,t & \cdots & \omega_{i_Nm_{2N-k}}\xi^2_{m_1}(0)\,t \\ \vdots & & \vdots & \vdots & & \vdots & \vdots & & \vdots \\ \xi^k_{j_1}(0) & \cdots & \xi^k_{j_{k-N}}(0) & \eta^k_{i_1}(0) & \cdots & \eta^k_{i_{k-N}}(0) & \omega_{i_{k-N+1}m_1}\xi^k_{m_1}(0)\,t & \cdots & \omega_{i_Nm_{2N-k}}\xi^k_{m_1}(0)\,t \end{vmatrix} \propto \frac{1}{t^k}\cdot t^{2N-k} \approx \frac{1}{t^{2(k-N)}}$$

Behavior of $GALI_k$ for regular motion

2D Hamiltonian (Hénon-Heiles system)

N=2

$$GALI_k(t) \propto \begin{cases} \text{constant} & \text{if } 2 \le k \le N \\ \dfrac{1}{t^{2(k-N)-m}} & \text{if } N < k \le 2N \text{ and } 0 \le m < k-N \\ \dfrac{1}{t^{k-N}} & \text{if } N < k \le 2N \text{ and } m \ge k-N \end{cases}$$

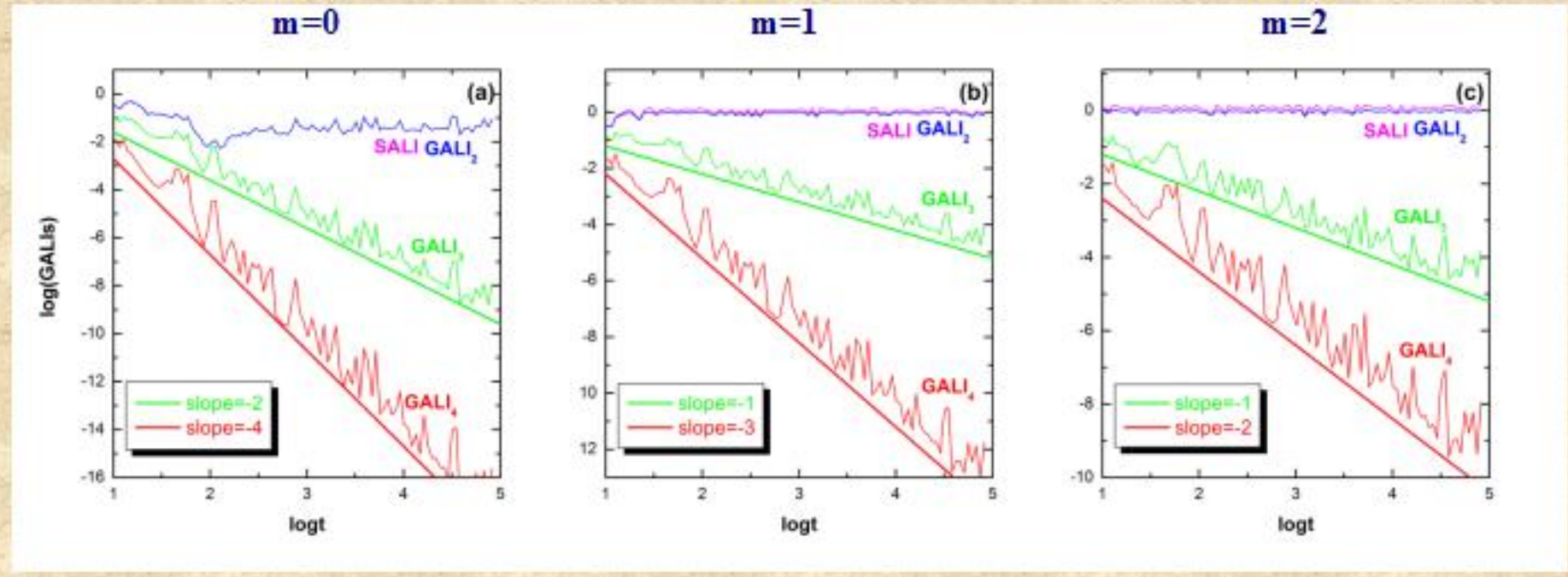

Behavior of $GALI_k$ for regular motion

3D Hamiltonian

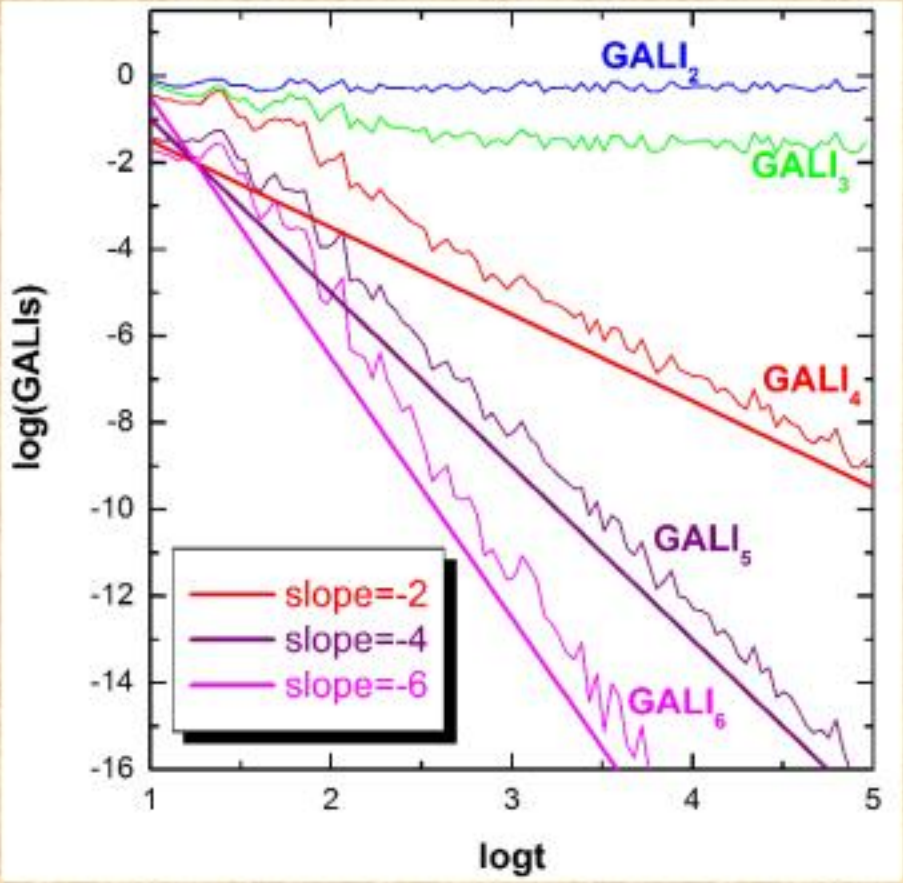

m=0

Behavior of $GALI_k$

Chaotic motion:

SALI→0 exponential decay

$$GALI_k(t) \propto e^{-[(\sigma_1-\sigma_2)+(\sigma_1-\sigma_3)+\ldots+(\sigma_1-\sigma_k)]t}$$

Regular motion:

SALI→constant ≠ 0 or SALI→0 power law decay

$$GALI_k(t) \propto \begin{cases} \text{constant} & \text{if} \quad 2 \le k \le N \\ \dfrac{1}{t^{2(k-N)-m}} & \text{if} \quad N < k \le 2N \text{ and } 0 \le m < k-N \\ \dfrac{1}{t^{k-N}} & \text{if} \quad N < k \le 2N \text{ and } m \ge k-N \end{cases}$$

Global dynamics

- $GALI_2$ (practically equivalent to the use of SALI)
- $GALI_N$

Chaotic motion: $GALI_N \to 0$ (exponential decay)

Regular motion: $GALI_N \to$ constant $\neq 0$

3D Hamiltonian

Subspace $q_3=p_3=0$, $p_2 \geq 0$ for t=1000.

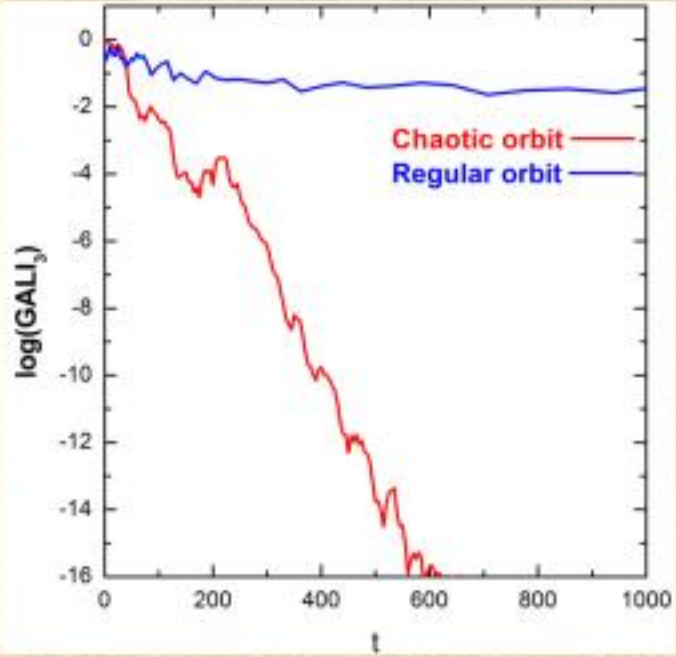

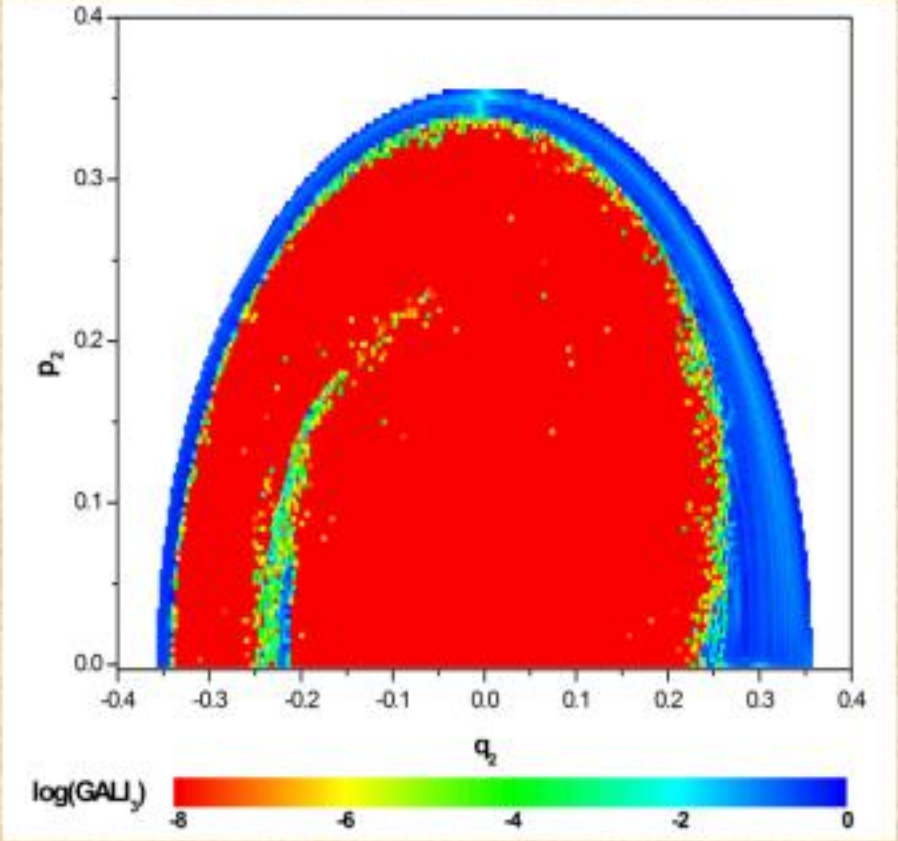

Global dynamics

$GALI_k$ with k>N

The index tends to zero both for regular and chaotic orbits but with completely different time rates:

Chaotic motion: exponential decay

Regular motion: power law

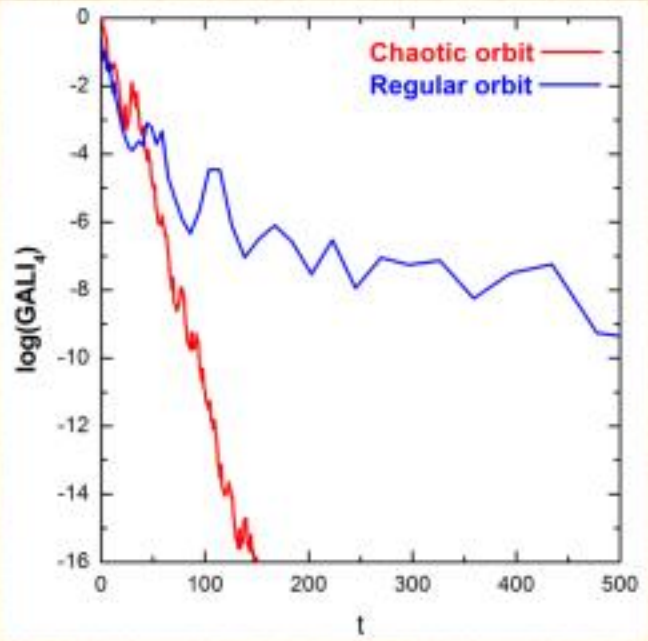

2D Hamiltonian (Hénon-Heiles)
Time needed for $GALI_4 < 10^{-12}$

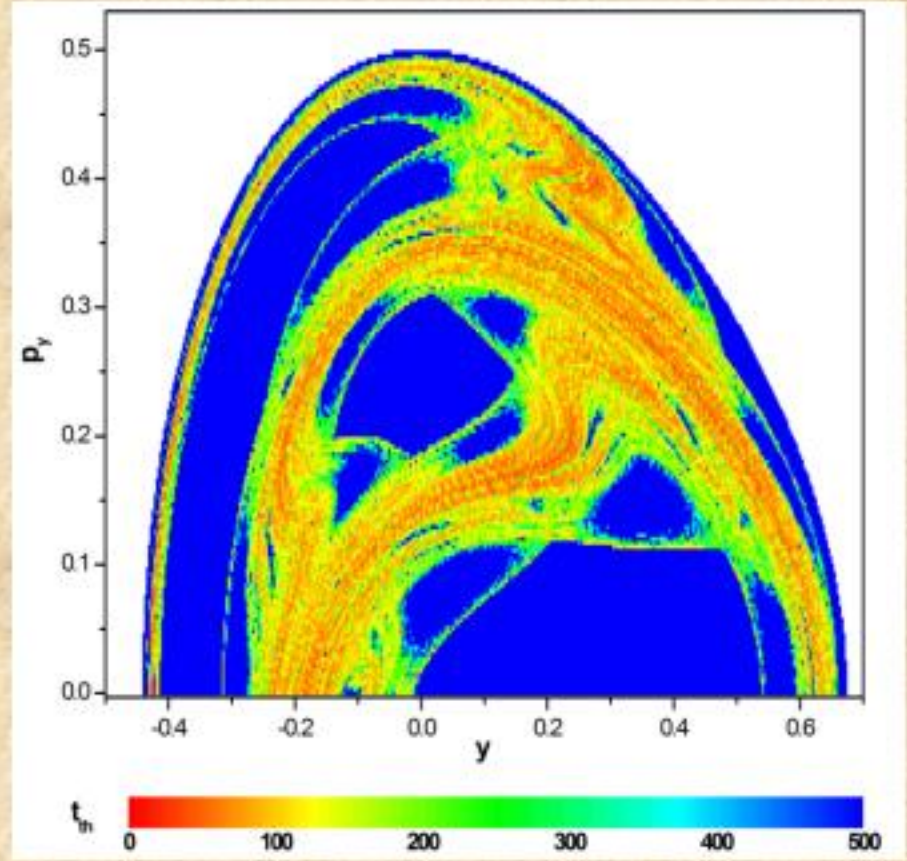

References - 1

- **Hamiltonian systems and symplectic maps**
  - ✓ Lieberman A. J. & Lichtenberg M. A. , 1992, Regular and Chaotic Dynamics, Springer.
  - ✓ Cvitanović P., Artuso R., Dahlqvist P., Mainieri R., Tanner G., Vattay G., Whelan N. & Wirzba A., 2004, Chaos – Classical and Quantum, http://chaosbook.org/
- **Lyapunov exponents**
  - ✓ Oseledec V I, 1968 *Trans. Moscow Math. Soc.* **19** 197
  - ✓ Benettin G, Galgani L and Strelcyn J-M 1976 *Phys. Rev. A* **14** 2338
  - ✓ Pesin Y B, 1977 *Russian Math. Surveys* **32** 55
  - ✓ Benettin G, Galgani L, Giorgilli A and Strelcyn J-M 1980 *Meccanica* **March** 9
  - ✓ Benettin G, Galgani L, Giorgilli A and Strelcyn J-M 1980 *Meccanica* **March** 21
  - ✓ Greene J M and Kim J-S *Physica D* **24** 213
  - ✓ Wolf A, Swift J B, Swinney H L and Vastano J A 1985 *Physica D* **16** 285
  - ✓ Bridges T J and Reich S *Physica D* **156** 219
- **Frequency Analysis**
  - ✓ Laskar J 1988 *Astron. Astrophys.* **198** 341
  - ✓ Laskar J 1990 *Icarus* **88** 266
  - ✓ Laskar J, Froeschle C and Celletti A 1992 *Physica D* **56** 253
  - ✓ Laskar J 1993 *Physica D* **67** 257
  - ✓ Dumas H S and Laskar J 1993 *Phys. Rev. Let* **70** 2975
  - ✓ Papaphilippou Y and Laskar J 1996 *Astron. Astrophys.* **307** 427
  - ✓ Papaphilippou Y and Laskar J 1998 *Astron. Astrophys.* **329** 451
  - ✓ Laskar J 1999 *Hamiltonian systems with three or more degrees of freedom* (ed. Simo C / Plenum Press) p 134
  - ✓ Robutel P and Laskar J 2001 *Icarus* **152** 4
  - ✓ Robutel P and Gabern F 2006 *MNRAS* **372** 1463

References - 2

- **SALI – GALI**
  - ✓ Skokos Ch 2001 *J. Phys. A* **34** 10029
  - ✓ Skokos Ch, Antonopoulos Ch, Bountis T C and Vrahatis M N 2003 *Prog. Theor. Phys. Supp.* **150** 439
  - ✓ Skokos Ch, Antonopoulos Ch, Bountis T C and Vrahatis M N 2004 *J. Phys. A* **37** 6269
  - ✓ Skokos Ch, Bountis T C and Antonopoulos Ch 2006 (submitted)
  - ✓ Szell A, Erdi B, Sandor Zs and Steves B 2004 Mon. Not R. Astron. Soc. **347** 380
  - ✓ Kalapotharakos C Voglis N and Contopoulos G 2004 Astron. Astroph., **428** 905
  - ✓ Manos T and Athanassoula E 2005 in '*SF2A-2005: Semaine de l' Astrophysique Française*', eds. Casoli F Contini T Hameury J.M and Pagani L, EDP-Sciences Conference Series, 631
  - ✓ Bountis T C and Skokos Ch 2006 *Nucl. Inst. Meth. Phys. Res. A* **561** 173
  - ✓ de Assis L P G Helayël-Neto J A Hass F and Nogueira A L M A 2006 Fifth International Conference on Mathematical Methods in Physics – IC2006, Proceedings of Science, PoS(IC2006)059
  - ✓ Capuzzo-Dolcetta R, Leccese L, Merritt D and Vicari A 2006 astro-ph/0611205
- **FLI**
  - ✓ Froeschle C, Lega E and Gonczi R 1997 *Celest. Mech. Dyn. Astron.* **67** 41
  - ✓ Froeschle C, Gonczi R and Lega E 1997 *Planet. Space Sci.* **45** 881
  - ✓ Fouchard M, Lega E, Froeschle Ch and Froeschle C 2002 *Celest. Mech. Dyn. Astron.* **83** 205
  - ✓ Guzzo M, Lega E and Froeschle C 2002 *Physica D* **163** 1
  - ✓ Barrio R 2005 *Chaos Sol. Fract.* **25** 71

References - 3

- **MEGNO**
  - ✓ Cincotta P M and Simo 2000 *Astron. Astroph. Suppl. Ser.* **147** 205
  - ✓ Cincotta P M, Giordano C M and Simo C 2003 *Physica D* **182** 151
- **RLI**
  - ✓ Sandor Zs Erdi B Szell A and Funk B 2004 *Celest. Mech. Dyn. Astron.* **90** 127
  - ✓ Erdi B and Sandor Zs 2005 *Celest. Mech. Dyn. Astron.* **92** 113
- **Dynamical spectra**
  - ✓ Froeschle C, Froeschle Ch and Lohinger E 1993 *Celest. Mech. Dyn. Astron.* **56** 307
  - ✓ Lohinger E, Froeschle C and Dvorak R 1993 *Celest. Mech. Dyn. Astron.* **56** 315
  - ✓ Voglis N and Contopoulos G 1994 *J. Phys. A* **27** 4899
  - ✓ Contopoulos G and Voglis N 1996 *Celest. Mech. Dyn. Astron.* **64** 1
  - ✓ Froeschle C and Lega E 1998 *Astron. Astroph.* **334** 355
  - ✓ Voglis N Contopoulos G and Efthymiopoulos C 1999 *Celest. Mech. Dyn. Astron.* **73** 211
  - ✓ Vozikis Ch L, Varvoglis H and Tsiganis K 2000 *Astron. Astroph.* **359** 386
- **Other methods**
  - ✓ Voyatzis G and Ichtiaroglou S 1992 *J. Phys. A* **25** 5931
  - ✓ Kotoulas T and Voyatzis G 2004 *Celest. Mech. Dyn. Astron.* **88** 343
  - ✓ Gottwald G A and Melbourne I 2004 *Proc. Roy. Soc. London A* **460** 603
  - ✓ Howard J E 2005 *Celest. Mech. Dyn. Astron.* **92** 219
  - ✓ Sideris I V 2006 *Phys. Rev. E* **73** 066217